

FINAL TECHNICAL REPORT

HOLOCENE GEOLOGIC CHARACTERIZATION OF THE NORTHERN SAN ANDREAS FAULT, GUALALA, CALIFORNIA

Recipient:

²William Lettis & Associates, Inc.
1777 Botelho Drive, Suite 262
Walnut Creek, CA 94596
Phone: (925) 256-6070; Fax: (925) 256-6076
www.lettis.com; baldwin@lettis.com

Principal Investigators:

Rich D. Koehler¹ and John N. Baldwin²

Contributors:

Carol S. Prentice³, and Justin Pearce²

¹Center for Neotectonic Studies
University of Nevada, Reno, MS 169
Reno, NV 89557
koehler@seismo.unr.edu

³U.S. Geological Survey
345 Middlefield Rd, MS 977
Menlo Park, CA 94025
cprentice@usgs.gov

Program Element I

Keywords:

Paleoseismology, geologic mapping, LIDAR, 1906 rupture

U.S. Geological Survey
National Earthquake Hazards Reduction Program
Award No. 03HQGR0045

November 2005

Research supported by U.S. Geological Survey (USGS), Department of Interior, under USGS award number 03HQGR0045. The views and conclusions contained in this document are those of the authors and should not be interpreted as necessarily representing the official policies, either expressed or implied, of the U.S. Government.

HOLOCENE GEOLOGIC CHARACTERIZATION OF THE NORTHERN SAN ANDREAS FAULT, GUALALA, CALIFORNIA

Award No. 03HQGR0045

Principal Investigators: Rich D. Koehler¹ and John N. Baldwin²
Contributors: Carol S. Prentice³, and Justin Pearce²

¹Center for Neotectonic Studies, University of Nevada, Reno, MS 169, Reno, NV 89557
koehler@seismo.unr.edu

²William Lettis & Associates, Inc., 1777 Botelho Drive, Suite 262, Walnut Creek, CA 94596
Phone: (925) 256-6070; Fax (925) 256-6076; www.lettis.com; baldwin@lettis.com

³U.S. Geological Survey, 345 Middlefield Rd, MS 977, Menlo Park, CA 94025; cprentice@usgs.gov

ABSTRACT

We performed detailed geomorphic mapping of active traces of the northern San Andreas Fault along a 24-km section in Mendocino and Sonoma Counties in northern California. Recently acquired airborne LIDAR data, encompassing a 70-km-long section of the fault, provided a powerful new tool for mapping geomorphic features related to the San Andreas Fault. This technique generates high-resolution images of the ground surface beneath the thick forest canopy that obscures much of the fault zone. Our collaborative effort with the U.S. Geological Survey represents the first use of LIDAR data to map active fault traces in a densely vegetated region along the northern San Andreas Fault. We interpreted shaded relief images generated from bare-earth DEMs and conducted detailed mapping of fault-related geomorphic features between the vicinity of Annapolis Road within the Gualala River basin and Voorhees Grove within the Garcia River basin. We initially mapped fault traces digitally, on-screen, based only on the geomorphology interpreted from LIDAR images, followed by field reconnaissance in order to verify and further refine our mapping along the entire 24-km length of the study.

The LIDAR imagery is an extremely valuable tool for field mapping in heavily forested areas and proved to be far superior to traditional mapping techniques relying only on aerial photography and 7.5 minute USGS topographic maps. Using the combined approach of office-based interpretation and field verification, we were able to significantly improve previous mapping efforts (Brown and Wolfe, 1972) along this rugged section of the fault and identified several sites suitable for future paleoseismic research. The final map products compiled in this study represent a more comprehensive survey of fault-related geomorphic features and the location of active traces of the fault. In conjunction with Carol Prentice of the U.S. Geological Survey, these maps will contribute to a new 70-km long strip map covering the entire on-land part of the northern San Andreas fault.

TABLE OF CONTENTS

ABSTRACT.....	i
1.0 INTRODUCTION	1
2.0 GEOLOGIC AND SEISMOTECTONIC SETTING.....	3
2.1 San Andreas Fault	3
2.2 Previous Mapping of the Northern San Andreas Fault	4
3.0 APPROACH AND METHODS	6
4.0 RESULTS	8
4.1 Quaternary/Holocene Deposits	8
4.1.1 Landslide Deposits.....	8
4.1.2 Fluvial Terrace Deposits.....	9
4.1.3 Small Scale Alluvial Deposits	10
4.2 Fault-related Features and Geometry of Active Fault Traces	10
4.2.1 Gualala River section.....	11
4.2.2 North Fork/Little North Fork Gualala River Section.....	12
4.2.3 Garcia River Section.....	14
4.3 Future Paleoseismic Research Site.....	16
6.0 ACKNOWLEDGMENTS	20
7.0 REFERENCES	21

LIST OF TABLES

Table 1. Geomorphic Symbol Codes used in Map Compilation	7
Table 2. Geomorphic Features along the Gualala River Section of the San Andreas fault (refer to Figures 6a-6e)	11
Table 3. Geomorphic features along the North Fork/Little North Fork Gualala River Section of the (refer to Figures 6f to 6h).....	13
Table 4. Geomorphic Features along the Garcia River Section of the San Andreas fault (refer to Figures 6i and 6j)	16

LIST OF FIGURES

- Figure 1. Regional map of the San Andreas fault in northern California, showing location of 1906 rupture, the North Coast segment of the fault, previous paleoseismic sites, area of this investigation, and the distribution of surface and geodetic slip produced by the 1906 rupture.
- Figure 2. Shaded relief map of the North Coast segment of the San Andreas fault between Valley Crossing in the Gualala River valley and Voorhees Grove in the Garcia River valley. Generalized faults from Brown and Wolfe (1972), shown within our 1-km wide mapping boundary. (Map compiled by Andrew Barron, University of Nevada, Reno).

- Figure 3. Northwest view from the vicinity of Fish Rock Road of the San Andreas fault in the middle foreground. The dense forest overstory makes the use of air photos in delineating fault related features difficult. The use of LIDAR imagery in this project eliminates the vegetative cover and allows for better delineation of fault-related geomorphology. Photo from (Wallace, 1990).
- Figure 4. Aerial photographs of the Garcia River valley showing dense vegetation and heavy modification by past logging operations along the northern San Andreas fault.
- Figure 5. Location map showing distribution of major drainages and place names along the northern San Andreas fault within the study area as described in text. Also shown are the boundaries of geomorphic description sections. Streams are either parallel to the northwest-trending fault rift valley or perpendicular to the fault.
- Figure 6. Active traces of the San Andreas fault compiled on a combined LIDAR and USGS topographic base map. Individual tectonic-related geomorphic features described in the field are numbered and labeled on the maps. Figures 6a, 6b, 6c, 6d, and 6e encompass the Gualala River section; Figures 6f, 6g, and 6h encompass the North Fork/Little North Fork Gualala River section; and Figures 6i and 6j encompass the Garcia River section.
- Figure 7. Location of geomorphic-related section boundaries along the 24-km-long field area of the San Andreas fault.
- Figure 8. Photograph, view to north-northeast, showing San Andreas fault at base of scarp on right adjacent to sag pond. Numerous large sag ponds exist along the fault in the Gualala River valley. A linear valley extends to the north.
- Figure 9. Photographs showing; A) redwood tree tilted on scarp of the 1906 rupture adjacent to large pond. B) close up of the base of tilted tree showing possible trunk deformation related to the 1906 rupture.
- Figure 10. Photographs showing dense brush within a narrow linear valley along the main trace of the San Andreas fault.

LIST OF CONTENTS ON CD

LIDAR images, “Bare-earth” model and “full-feature” model
 Digital USGS 1:24,000 scale quadrangles (DRG’s)
 Brown and Wolfe (1972) lineaments and geomorphic features
 Office based on-screen lineament interpretation
 Field verified lineament compilation and geomorphic features

1.0 INTRODUCTION

The northern San Andreas fault is one of the most prominent tectonic features along the western boundary of the North American plate and extends approximately 470-km from San Juan Bautista to Shelter Cove within the California Coast Range geomorphic province (Figure 1). The 470-km-long reach of the San Andreas fault last ruptured in 1906 as the devastating great San Francisco earthquake, which produced over 400-km of surface rupture on the fault (Lawson, 1908; Prentice et al., 1999) (Figure 1). Contrasting models aimed at assessing future large magnitude events on the northern San Andreas fault include, a characteristic rupture model where the fault ruptures in similar-sized 1906-type earthquakes, and a model in which the fault ruptures on discrete, smaller fault segments within the northern San Andreas fault. For instance, the Working Group on California Earthquake Probabilities (WGCEP, 2003) recognizes the possibility that the northern San Andreas fault may be composed of four separate rupture segments - Santa Cruz Mountains, Peninsula, North Coast and Offshore - that may have distinct rupture histories differing from large 1906-like events. To test rupture segmentation models it is necessary to compare earthquake recurrence and timing data from multiple sites along the fault. Turbidite event stratigraphy inferred to be related to earthquakes on the San Andreas fault is presently being developed offshore of the entire northern San Andreas fault (Goldfinger, 2000; 2001; and 2003a). Despite paleoseismic efforts in the study region (Prentice, 1989; Baldwin, 1996; Baldwin et al., 2000; Simpson et al., 1996; Noller et al., 1993; Prentice et al., 2000; 2001; Kelson et al., 2003; Kelson et al., 2005) on-land data on the recurrence and timing of events on the fault remain poorly constrained and no paleoseismic data exist within the rugged and forested Gualala River valley (Figure 2).

We performed geomorphic mapping, in collaboration with Dr. Carol Prentice of the U.S. Geological Survey, along a 24-km-long section of the North Coast segment between the vicinity of Annapolis Road (~6-km north of Stewarts Point) and Voorhees Grove (~8-km southeast of Point Arena) (Figure 2). The purpose of the study was to: (1) delineate and initially characterize active fault strands and fault-related geomorphology, (2) revise Brown and Wolfe's (1972) strip map, and (3) identify promising paleoseismic research sites to critically evaluate existing rupture models for the northern San Andreas fault. The identification of these sites and future assessments of earthquake history at these sites will provide a means to compare the offshore and on-land event record as well as provide an essential first step in developing data on earthquake timing, recurrence, and slip rate. These data will eventually contribute to estimating the probability and size of future earthquakes in the San Francisco Bay area and North Coast region.

Previous mapping of the North Coast section by Brown and Wolfe (1972) relied primarily on the interpretation of aerial photography, field reconnaissance, and compilation of geologic data onto 7.5-minute U.S. Geological Survey (USGS) topographic maps. The level of accuracy of these strip maps was limited by the rugged topography and are better suited for detailed geomorphic mapping, lack of topographic detail and control on 7.5 minute maps, and thick forest canopy which obscures tectonic-related geomorphology, making traditional mapping techniques (e.g., aerial photography interpretation) difficult. Thus, in this study we utilized new high resolution LIDAR (Light Distance and Ranging) data collected by NASA to eliminate the vegetative cover, and to develop "bare-earth" digital elevation maps that closely reflect the "hidden" topography. Similar high-resolution LIDAR topographic surveys have been successfully used in the Puget Lowlands of Washington to identify topographic scarps (e.g. Toe Jam Hill fault scarp; Waterman Point fault scarp) by imaging through the vegetative cover (Haugerud et al., 2001; Bucknam et al., 1999). These images were used to delineate fault scarps, offset streams, ponds, and faulted glacial deposits, as well as identify potential paleoseismic research sites. Subsequent paleoseismic trenching at these sites have successfully determined earthquake chronologies (Nelson et al., 2003; Johnson et al., 2004) that otherwise might have gone undetected using conventional mapping techniques (i.e., aerial photography and USGS topographic maps). Our efforts represent the first application of

LIDAR data to document the location of active traces of the northern San Andreas fault in the heavily forested Gualala and Garcia River basins in Northern California. These maps will provide a basis for guiding future paleoseismic research on the fault.

2.0 GEOLOGIC AND SEISMOTECTONIC SETTING

Our mapping area lies along a 24-km-long section of the roughly 190-km-long North Coast segment of the San Andreas Fault (Figures 1 and 2). The North Coast segment extends from Point Arena on the north to a complex intersection with the San Gregorio fault in the offshore area west of the Golden Gate (WGCEP, 2003; Figure 1). The portion of the fault mapped as part of this study lies northwest of Stewarts Point and southeast of Point Arena. Between Fort Ross and Point Arena and along the San Andreas fault, rocks of the Gualala block are faulted on the west against Franciscan Assemblage rocks on the east. The Gualala block consists of Cretaceous and Paleogene marine turbidites and nonmarine sedimentary rocks overlain by Neogene deposits of the Point Arena basin (Prentice, 1989; Loomis and Ingle, 1994). Pleistocene marine terrace deposits lie west of the field area and unconformably overlie Point Arena basin deposits. Franciscan Assemblage rocks east of the fault consist of Mesozoic marine sandstone and shale. Holocene fluvial and alluvial deposits of the Gualala and Garcia River Basin are partly constrained to the San Andreas Rift Zone.

2.1 San Andreas Fault

The North Coast segment of the San Andreas fault last ruptured in 1906 and currently is aseismic or nearly so (Hill et al., 1990). Previous workers have interpreted this relative lack of seismicity as evidence that the fault is "locked", and actively storing elastic strain energy for release in a future large-magnitude earthquake. The history of earthquakes along the North Coast segment is a critical element for probabilistic hazard assessments for the San Francisco Bay area. Models developed to explain the fault behavior have evolved through time and reflect the continuing advancement in paleoseismic data along the fault. For instance, the WGCEP (1990) assumed that the North Coast segment ruptures as a single segment, mainly because of a lack of data suggesting otherwise. However, subsequent compilation of surface observations with geodetic modeling indicate that the part of the North Coast segment between Point Arena and Fort Ross experienced a lower amount of slip during the 1906 earthquake than other parts of the rupture (Lawson, 1908; Thatcher et al., 1997) suggesting a sub segment boundary may be present along this section of the fault. For instance, variations in amount of geodetic slip along the fault estimated by these workers are similar to observed variations in surface offsets (i.e., offset fences, tree lines) documented by Lawson (1908). Geodetic and surface measurements suggest a smaller amount of slip in the Fort Ross area than elsewhere along the North Coast segment (Figure 1). These observations (see WGCEP, 2003) are particularly relevant to the most recent interpretations of rupture segmentation of the San Andreas Fault. If the North Coast segment typically ruptures in 1906-type events, with similar distributions of coseismic slip along the fault, then a "slip deficit" would develop in the Fort Ross area (Schwartz et al., 1998). In this scenario, additional smaller magnitude (e.g., $M_w \leq 6.9$) earthquakes would be required near Fort Ross, in order to satisfy the long-term slip budget of the fault. The WGCEP (2003) considered the possibility of a smaller earthquake in the Fort Ross area through inclusion of a floating, M_w 6.9 earthquake anywhere along the 470-km-long segment that ruptured in 1906.

Previous paleoseismic investigations assessing slip rate on the North Coast segment support the "slip-rate" deficit model along this section of the fault. Paleoseismic investigations at Point Arena (Prentice, 1989) and Olema (Niemi and Hall, 1992), suggest geologic slip rates of 23 ± 3 mm/yr and 24 ± 3 mm/yr, respectively, whereas studies near Fort Ross (Noller et al., 1993; Noller and Lightfoot, 1997; Prentice et al., 2001) suggest a preliminary rate of 19 ± 4 mm/yr. If this is the case, additional smaller magnitude (e.g., $M_w \leq 6.9$) earthquakes near Fort Ross may be necessary in order to satisfy the long-term slip budget of the fault. The intent of our study, in part, is to continue to test this model by identifying more favorable sites for slip rate assessments.

The recurrence of past earthquakes on the North Coast segment is estimated from the occurrence of at least five surface-rupturing earthquakes during the past 2,000 years near Point Arena (Prentice, 1989), and the occurrence of at least seven surface ruptures within the past 2,000 to 2,500 years at Vedanta (Figure 2; Niemi et al., 2002). Knudsen et al. (2002) interpret geologic evidence for changes in land surface elevation indicating the occurrence of three events within the past thousand years or so at Bolinas Lagoon and Bodega Bay (Figure 1), but note that present-day paleoseismologic and age-dating techniques are inadequate for differentiating between large earthquakes and temporally clustered smaller ruptures. Collectively, the numerous event chronology studies on the northern San Andreas fault indicate a range in recurrence for large earthquakes on the North Coast segment of the San Andreas fault of 180 to 370 years (WGCEP, 2003). Recent research on offshore turbidite sequences along the northern San Andreas fault document the occurrence of five episodes of turbidite deposition within the past thousand years. These turbidite sequences are interpreted to represent five paleoearthquakes that may be associated with large magnitude earthquakes on the Offshore and North Coast segments of the San Andreas Fault (Goldfinger et al., 2003). To help reduce the uncertainty in characterizing the rupture behavior of the northern San Andreas fault, further refinement of the chronology of large surface ruptures and slip rate variability along the fault is needed.

2.2 Previous Mapping of the Northern San Andreas Fault

Our mapping area between the vicinity of Annapolis Road (~6 km north of Stewarts Point) and Voorhees Grove (~8 km southeast of Point Arena) includes a region of the North Coast segment of the San Andreas fault that intersects rugged, mountainous terrain (Figures 2 and 3). A significant portion of the map area is privately owned by logging companies which over the decades have logged sections of forest along the length of the fault zone. Aerial photographs are of limited use along the Gualala and Garcia River valleys due to the dense cover of conifer overstory (Figure 4). Additionally, due to limited private land access and rugged terrain along the North Coast segment of the San Andreas fault much of the geomorphic evidence of the 1906-rupture is poorly documented. Available accounts of the rupture are limited to Lawson (1908), who also found this stretch of the fault logistically demanding, and Brown and Wolfe (1972) who provide an initial characterization of 1906 fault-related geomorphic features and locations of fault strands. These maps were the basis for Alquist-Priolo special study zone maps for the San Andreas fault produced by the California Geological Survey.

On the basis of our review of initial fault mapping by Brown and Wolfe (1972) between Point Arena and Fort Ross, the North Coast segment of the San Andreas fault is characterized by relatively short en echelon, overlapping fault splays typically one to three kilometers long (Figure 2). From southeast to northwest through the map area, the San Andreas fault traverses long, linear, shallow gradient valleys that contain the Gualala, North Fork Gualala, Little North Fork Gualala, South Fork Garcia, and Garcia Rivers (Figures 2 and 5). The long linear channels of these rivers indicate long term fluvial adjustment to offset along the fault and stream pirating processes. Because the location of the fault is on the southwestern valley wall in both the Gualala and Garcia River valleys, it intersects many small tributary streams. The fault has altered the course of many of these streams, as well as deposition of sediment within them. Brown and Wolfe (1972) noted that major fault breaks of the 1906 rupture were evident on aerial photographs as natural openings and lineaments in the second growth forest. On the ground these openings were found to be natural meadows, swamps, or ponds occupying depressions, and were interpreted as fault-related features (Brown and Wolfe, 1972). Brown and Wolfe (1972) also noted that the recognition of offset streams and other relatively subtle topographic or drainage features that help delineate the fault were inhibited by the forest cover. Although these previous mapping efforts provide an initial assessment of fault location, style of surface faulting, and evidence for the 1906 rupture, they do not provide information on small-scale tectonic-related geomorphic lineaments that are necessary for evaluating potential paleoseismic research sites, and better characterizing the active fault trace(s). Other available maps for the Gualala area include bedrock mapping by Wentworth (1966). However, the

mapping performed by our study greatly improves upon these maps which were made by traditional aerial photography analysis and relied upon 7.5 minute USGS topographic maps.

3.0 APPROACH AND METHODS

Our approach to using LIDAR images to map active traces of the northern San Andreas fault includes office-based and field-based methods. Our mapping strategy was to first, compile existing data on fault location and character of geomorphic features related to faulting (i.e. Brown and Wolfe, 1972). Secondly, we interpreted and compiled fault traces (e.g. lineaments) digitally, on-screen, based on geomorphology interpreted from shaded relief images generated from bare-earth LIDAR images. Finally, we conducted field reconnaissance using prints of the initial computer-based maps in order to verify the lineaments with respect to location and tectonic origin.

LIDAR images were uploaded to a GIS program (ARCMAP) which was used to interpret and compile fault related features on-screen. Lineaments suspected of tectonic origin were color coded based on inferred relative age, such as: 1906 (red), Holocene (orange), Quaternary (purple), and unknown lineaments (black) (see enclosed CD). We then created an ARCMAP coverage built around the LIDAR images using various base layers including digital 1:24,000-scale USGS topographic quadrangles (DRG's), and 30-m and 90-m digital elevation models (DEM's). Digital maps depicting geomorphic features in the Gualala River watershed were reviewed and acquired from the California Geological Survey. We digitized fault-related geomorphic features and interpreted locations of fault strands associated with the 1906 rupture from maps completed by Brown and Wolfe (1972). Additionally, we were provided a digital database including streams and dirt roads from Gualala Redwood Company and Mendocino Redwood Company. The road maps were overlain on the LIDAR prints to assist us in field locating and driving. The digital database described above was used to compare lineaments interpreted on LIDAR to previously published fault location maps in an effort to more accurately map the fault.

Our LIDAR lineament interpretation was field checked by systematically walking the fault from south to north between the vicinity of Annapolis Road and Voorhees Grove, respectively. The LIDAR data proved invaluable (far superior to aerial photographs) for accurately locating fault strands and other geomorphic features. In the field, we used two versions of the LIDAR data (1:6,000-scale) including: (1) a "full-feature" model that incorporates the distribution of vegetation, and (2) a "bald-earth" model that shows detailed topography void of vegetation. By cross comparing the LIDAR data to aerial photographs and topographic maps we were able to confidently locate and document tectonic features on the map. Geomorphic features such as, scarp height (estimated) and orientation, sag ponds, offset streams, shutter ridges, and linear valleys were noted and photographed in the field and incorporated into the GIS as a point coverage with data tables describing each feature. Geomorphic features were designated on the maps using the symbols listed in Table 1. Lineaments (inferred faults) interpreted from the LIDAR data were classified in the field, based on prominence of tectonic related geomorphology, into four class designations, including strong evidence (solid line), distinct evidence (long dash line), weak evidence (short dash line), and concealed (dotted line). In addition, a few lineaments interpreted as potential fault strands during our office compilation were determined in the field to be of cultural origin (roads, powerlines, skid trails) and not of tectonic origin. These were noted in the field and removed from the final digital fault map.

The entire 24-km reach of the fault between the vicinity of Annapolis Road and Voorhees Grove was field verified. This included mapping landslide, fluvial, and alluvial deposits to provide guidance on the differentiation between landsliding and tectonic-related geomorphology, and to assess the stratigraphy of potential paleoseismic research sites. Because landslide deposits and high erosion rates sometimes obscure or remove youthful geomorphic expression of faulting, the active fault traces depicted on our final map represent interpretations of multiple sources of data that may or may not indicate the location of the 1906 rupture. However, we believe, collectively the data provide sufficient evidence to make

reasonable judgments regarding the viability of future research sites and the likely location of future fault rupture on the North Coast segment of the San Andreas fault.

Table 1. Geomorphic Symbol Codes used in Map Compilation

Geomorphic Feature	Symbol
Scarp (northeast facing)	s (NE)
Scarp (southwest facing)	s (SW)
Pond	p
Swampy depression	ds
Dry linear depression or swale	d
Saddle	sa
Spring	sp
Linear valley	lv
Linear drainage	ld
Swale	sw
Linear break in slope	bs
Bench	b
Tectonic ridge	r
Stream knickpoint	kp
Vegetation lineament	v
Drainage divide	dd
Offset stream channel	os
Beheaded or abandoned stream channel	bs
Deflected stream	ds
Pirated channel	pc

4.0 RESULTS

As a result of our mapping of this 24-km-long section of the northern San Andreas fault we have delineated fault related geomorphology and the location of active fault traces within three geographically distinct sections. From southeast to northwest these sections include the: Gualala River Section, North Fork/Little North Fork Gualala River Section, and the Garcia River Section (Figure 5). Additionally, we have evaluated the distribution of landslide, fluvial, and alluvial deposits along the active fault trace, and identified a very viable potential paleoseismic research site. Our results indicate that the greatest number of potential paleoseismic research sites occur along the North Fork/Little North Fork Gualala River section of the fault. Along this stretch of the fault, we identified multiple sites where Holocene deposits provide cover and stratigraphy suitable to paleoseismic research. Because of access constraints (i.e. absence of roads, presence of thick vegetation, and/or deep stream valleys) associated with many of these sites, we focus our attention on one site that is readily accessible by a recently cleared logging skid trail (see below). Lastly, our mapping also suggests that a kinematic fault segment boundary may potentially exist between the North Fork/Little North Fork Gualala River Section and the Garcia River Section based on geomorphic relations along this stretch of the fault.

4.1 Quaternary/Holocene Deposits

4.1.1 Landslide Deposits

In the natural forest environment of the Garcia and Gualala River basins, mass wasting is a common occurrence due to relatively steep slopes, deep weathering of the Franciscan and Tertiary bedrock, thick colluvial soils, and the occurrence of high intensity winter rainfall events. Mass wasting, therefore, plays a major role in developing the morphology of the steep, mountainous terrain. Landslide deposits along the mapped trace of the San Andreas fault include shallow landslides, debris flows, and deep seated landslides (earthslumps and earthflows). In places, these deposits have obscured or obliterated geomorphic evidence of the fault location. A comprehensive detailed depiction of landslides was not included on our final map, because (1) landslides are rarely useful in assessing the location of the fault; (2) landslides are abundant in areas away from the fault where we focused our field efforts; and (3) 1:24,000 scale landslide mapping was not part of the scope of this project. However, we were careful to not confuse landslide- related lineaments and geomorphology from similar looking fault-related features. Detailed maps depicting the location of hundreds of modern landslides (last 50 years) have been compiled by Mendocino Redwood Company and Gualala Redwood Company as part of watershed analysis studies in the Garcia and Gualala River watersheds, respectively (Surfleet and Koehler, 1998; Best, 1997). We reviewed these and the location of landslides relative to our interpreted fault lineament mapping. Additionally, refer to the “Geomorphic Features related to landsliding map series” and “Watershed Mapping Series” for detailed landslide maps in the region (Spittler, 1982; CGS, 2003). We provide brief descriptions of the types and character of landslide deposits below.

Shallow landslides are the most common landslides in the study area and occur primarily on steep inner gorge slopes, steep side slopes and over-steepened road fill. These slides include debris avalanches, rock falls, and landslides involving colluvium/soil. Shallow landslide widths at the headscarp range from about 3 to 70 m and the deposit can be up to 100 m in length. We recognized shallow landslide deposits in the field by talus accumulation at the base of slopes, or by hummocky, irregular surfaces on hillslopes. We did not observe any shallow landslides offset by the fault during our field mapping. At a few localities, however, shallow landslide deposits within narrow linear valleys were observed to cause ponding and alluvial deposition against the fault scarp.

Debris flows are characterized by a highly mobile slurry of soil, rock, vegetation, and water that can travel many miles down steep confined mountain channels (Varnes, 1958). Debris flows within the study area are initiated in deep colluvial hollows along first order streams and/or concave slopes where ground and surface waters tend to concentrate. Debris flow deposits are massive, poorly sorted, and are often preserved as in-channel debris fans. We did not observe any debris flow deposits offset by the fault.

Within the map area, deep seated landslides occur primarily along the southwestern valley slope of the Gualala and Garcia Rivers (Brown and Wolfe, 1972; Spittler, 1982). These features include earth slumps and earthflows characterized by hummocky topography and rotational failures characterized by back rotation along a concave failure surface. Brown and Wolfe (1972) mapped two deep seated slides that show possible evidence of right lateral displacement. One of these slides occurs ~1 km northwest of the confluence between the South Fork Garcia and Garcia Rivers at Voorhees Grove. Based on Brown and Wolfe map, this slide appears to have deflected the course of the Garcia River. Our field reconnaissance noted a high fluvial terrace (35 meter elevation) developed into their landslide deposit suggesting that the slide is at least Quaternary age and has been relatively stable since that time. Additionally, we were unable to define the margin of this slide in the field and were, thus, unable to confirm that the landslide was offset along the fault. The second deep seated landslide that shows possible offset lies along Fish Rock road at the drainage divide between the Little North Fork Gualala and South Fork Garcia Rivers. This slide exhibits prominent hummocky topography southwest of the fault. The apparent offset of this landslide deposit is about 500 m, however, this offset could also be the result of incision of the Little North Fork Gualala River headwater channel or primary deposition. Large uphill facing scarps have developed along the fault across both of these landslides suggesting a long period of relative stability and a Quaternary age. Because the exact age of these deposits is unknown, they are not useful in determining slip rate information. Other deep seated landslides mapped by Brown and Wolfe either do not cross the fault or do not show right lateral offset in plan view.

We identified one deep seated landslide that was not documented by Brown and Wolfe (1972). This landslide occurs approximately 400 m southwest of the confluence between the South Fork Garcia and Garcia Rivers. This slide is characterized by hummocky topography, smaller shallow landslides within the slide mass, and displaced bedrock blocks. Fault related geomorphology across the slide includes active springs and ponded water. Recent movement of the slide mass has modified other fault related geomorphology and we were unable to identify a tectonic-related scarp traversing the slide. Because of the modification of tectonic-related geomorphology we did not consider this area to be conducive to future paleoseismic studies.

4.1.2 Fluvial Terrace Deposits

Quaternary and Holocene fluvial terrace deposits exist throughout the mapping area and consist of unconsolidated gravels and boulders supported by silty sand matrix. Late Quaternary deposits occur as highly dissected remnants preserved along the valley slopes and within the drainage divide between the Garcia and Gualala River systems. These deposits are difficult to recognize in the field because of their dissected form and thick vegetative cover, however, outcrops can occasionally be found along incised tributary stream channels.

Holocene fluvial terraces occur along the lower reaches of every major tributary stream and along the trunk rivers that follow the San Andreas fault rift valley. These terraces lie at various elevations and the lowest terrace surface is about 2.5 to 3 m above gravel bars that flank the modern channel. The modern terrace surface experiences sand and silt deposition during large flood events, but is abandoned most of the year. The fault traverses Holocene terrace deposits along the Little North Fork, North Fork, and South Fork Gualala Rivers and is usually expressed as a subtle southwest facing scarp 0.5 to 1.5 m high. Streams that drain across Holocene terrace deposits have been deflected along the fault. Terrace deposits

and the river parallel the fault and were not observed to cross the fault at a high angle. Therefore, our geologic and geomorphic mapping did not identify any places along the fault where it intersects terrace backedges that may be favorable for slip rate or slip-per-event studies.

Elk Prairie is a 300 meter wide Holocene terrace surface located at the confluence of the Little North Fork and North Fork Gualala Rivers. Deposits beneath this surface consist of 55 m of alternating layers of blue clay, gravel, and reddish brown silt (CGS, 2003). Based on this information, CGS (2003) inferred that during times when sea level rise was synchronous with uplift, gravel was deposited in a low gradient stream; whereas during times when sea level rise exceeded uplift, clay was deposited in an estuary environment. The modern terrace surface was probably incised when the rate of Holocene sea level rise slowed in the mid-Holocene. A similar depositional history may be associated with Holocene terrace deposits along the South Fork Gualala River, however subsurface data does not exist (CGS, 2003).

4.1.3 Small Scale Alluvial Deposits

Small scale alluvial deposits exist locally along the fault and include, pond deposits, alluvial fan deposits, and fluvial deposits. The aerial extent of these deposits typically were too small to show at the 1:24,000 scale mapping, but were identified at specific sites for the purpose of assessing the presence of Holocene bedded material suitable for preserving earthquake chronology data. The majority of the elongate ponds found along the fault are not true sag ponds where the pond exists between stepping strands of the fault. Instead, the ponds are the result of long term horizontal offset that has created local closed depressions. Southwest facing scarps have trapped streamflow from northeast oriented streams and created the elongate ponds. Sediment within the ponds generally consists of dark brown to black organic rich silt that may or may not be interbedded with thin alluvial fan and fluvial deposits in the subsurface. In areas where the southwestern side of the fault is not ponded, alluvial fan and fluvial deposits locally onlap the scarp. Alluvial fan deposits consist of angular gravels and boulders in a sandy silt matrix. These deposits create local drainage divides and contribute to the closed depression morphology southwest of the fault. Fluvial deposits consist of rounded gravels and sand. These deposits are most common where steep headwater streams intersect flat terrace surfaces causing the stream to meander and deposit sediment. The specific locations of pond, alluvial fan, and fluvial deposits are shown in our geomorphic feature point coverage described below.

4.2 Fault-related Features and Geometry of Active Fault Traces

From south to north, the fault traverses the southwestern valley slope of the linear South Fork Gualala and main Gualala Rivers, extends along the channel of the North Fork Gualala River, and traverses the southwestern valley slopes of the Little North Fork Gualala, South Fork Garcia, and Garcia Rivers (Figures 2 and 5). To simplify the description of active fault traces and fault-related geomorphology, we separate the fault into three distinct geographic zones herein referred to as: (1) the Gualala River section; (2) the North Fork/Little North Fork Gualala River section; and (3) the Garcia River section (Figure 5). We emphasize that these section names are used herein only for descriptive purposes and should not be interpreted as representing actual fault rupture segments or boundaries. Because regionally named watercourses are the only feature of reference, we describe each map section by referring to creek names shown on Figure 5 for location clarity. Active fault strands and tectonic-related geomorphic features described in the text are shown on Figures 6a-6j, and a complete view of the fault geometry through the study area is shown on Figure 7.

Within the map area the fault is geomorphically expressed as short overlapping fault splays and parallel, linear ridges and swales. The linear ridges are oriented along fault traces that alternate between a single main trace and zones of left-stepping fault traces. Uphill facing ridges are often associated with linear valleys and large ponds. Numerous notches and abandoned channels cut through the uphill facing ridges.

At these localities, the paleodrainages are partially filled with colluvial and alluvial sediment and are traceable across the topography. Alluvial fans sourced from small east-flowing ephemeral streams create local drainage divides where the fans are deposited against the scarp and streams are diverted northwest and southeast along the fault. These features are common throughout the entire map area and possess site conditions and stratigraphy that may have potential to reveal timing and recurrence information from future paleoseismic investigations. Below, from southeast to northwest, we discuss in more detail specific geomorphic relations encountered along the fault zone.

4.2.1 Gualala River section

The Gualala River section is shown on Figure 5 and Figures 6a to 6e and extends from the southern property boundary of Gualala Redwood Company (~3 km south of Annapolis Road) to the vicinity of Big Pepperwood Creek. The most common fault related geomorphic features along this section are left stepping en echelon pattern of fault splays and large ponds bordered by southwest facing scarps.

Along the southern part of the Gualala River section, the fault extends along the northeast facing valley slope along the southwestern side of the Gualala River, north to the vicinity of Buckeye Creek. In this area, the fault consists of left stepping, en echelon strands ranging in length from about 0.8 to 2.4 km long that traverse a prominent linear sidehill fault valley. At the fault stepovers, individual strands have overlaps ranging from about 150 to 500 m. Eight large ponds (~200 to 300 m long) and numerous small ponds and swampy bogs are impounded against uphill (southwest) facing scarps along this section (Table 2, Figures 6a-e and 8). The scarps range in height from about 2-15 m (avg. ~5-6 m) and are relatively continuous from the map boundary to the vicinity of Buckeye Creek (Table 2, Figures 6a-d). Evidence of continued right lateral offset along the fault is in the form of offset stream channels that cut through the scarp(s) and remnant stream channels (abandoned) that cut east-west across the scarp(s) (Table 2). The topographic relief within the fault valley is relatively flat, however numerous subtle drainage divides exist that separate the streamflow direction into northwest and southeast flowing sections and contribute to the formation of the large ponds. Because the ponds along this section are large and densely vegetated, and would pose access constraints and dewatering logistics, we do not feel they represent good future paleoseismic research sites at this time.

Table 2. Geomorphic Features along the Gualala River Section of the San Andreas fault (refer to Figures 6a-6e)

Location	Geomorphic Feature	Site Number
~ 3 km south of Annapolis Road to Buckeye Creek	Ponds and swampy bogs	1, 2, 6, 8, 11, 12, 16, 21, 22, 23, 24, 26, 28, 30, 31, 33, 35, 39, 45, 47, 50, 59, 70, 72, 74, 75, 79, 81
~ 3 km south of Annapolis Road to Buckeye Creek	Scarps	36, 40, 42, 48, 49, 52, 54, 61, 77, 86, 87, 90, 92, 94
~ 3 km south of Annapolis Road to Buckeye Creek	Offset streams and beheaded channels	3, 4, 5, 7, 9, 10, 20, 27, 32, 34, 55, 56, 64, 69, 71, 84, 85, 93
Buckeye Creek to Big Pepperwood Creek	Ponds and swampy depressions	96, 99, 103, 110, 119, 120, 137
Buckeye Creek to Big Pepperwood Creek	Scarps	97, 99, 101, 102, 104, 110, 115, 122, 123, 124, 126, 129, 134, 142
Buckeye Creek to Big Pepperwood Creek	Offset streams and beheaded channels	116, 118, 125, 136, 142, 144

North of Buckeye Creek to the vicinity of Big Pepperwood Creek (Figures 6d and 6e), the fault extends along the back edge of the lowest prominent Holocene river terrace and along the base of the southwest valley wall adjacent to the Gualala River. In this section, the geomorphic expression of the fault becomes more subtle. In places where the fault lies along the edge of the river, active erosion during flood flows has removed or obscured fault-related features, leaving landslide debris slopes. Where the fault extends across the Holocene fluvial terrace on the southwest side of the river, it is characterized by small southwest facing scarps, small oval shaped closed depressions, moisture dependent vegetation (i.e. pampas grass and skunk cabbage), and linear swales (Sites #134-143, Figure 6e). Stream channels that drain the southwest valley slope meander across the terrace of the Gualala River and exhibit a right angle drainage pattern (bend northwest and southeast) where the streams intersect the fault. Scarps in this area are smaller than scarps to the south and range from about 0.5 to 1.5 m in height. Fault morphology has been modified along short sections where old logging skid trails and logging roads parallel the fault trace. In contrast to the left-stepping, en echelon pattern observed to the south, the fault appears to be a single fault trace with an orientation between N35°-45°W (Figures 6d, 6e, and 7). A few short splay faults branch off west of the main trace, but are only continuous for a few hundred meters. A zone of right stepping fault splays and an overall northeast bend in the Gualala River characterizes the northern end of the Gualala River section (Figures 6e and 7). This right bend may represent either a sinuous fault trace or a fault asperity related to a subtle change in orientation of the fault trace. The location of selected geomorphic features along this stretch of the fault are listed in Table 2 and shown on figures 6d and 6e.

Potential paleoseismic study sites where alluvium is ponded against a fault scarp along the section between Buckeye Creek and Big Pepperwood Creek includes sites #101, 117, and 129 (Figures 6d and 6e). At site #101, alluvium is ponded against a short prominent western fault splay, deposited across the northern end of the western splay, and is ponded against an eastern splay where it intermittently is flooded by a pond to the north. Site #117 has bedded alluvium composed of lithologies derived from the west ponded against a small scarp in a terrace deposit that consists of Franciscan gravels derived from the east (Figure 6d). Site #129 consists of a sidehill bench across a landslide deposit at the mouth of a tributary drainage (Figure 6d). The landslide deposit appears to be offset up to the northeast ~1 m. Although these three sites have paleoseismic potential, we feel that the unknown amount of historic modification and the amount of logging slash and brush clearing that would be necessary to access these sites, severely limits their viability to produce robust paleoseismic results.

4.2.2 North Fork/Little North Fork Gualala River Section

The North Fork/Little North Fork Gualala River section extends from the vicinity of Big Pepperwood Creek to the drainage divide with the Garcia River basin (Figure 5 and Figures 6f, 6g, and 6h). Approximately 500 m north of Big Pepperwood creek, the fault projects across the Gualala River and extends across the front edge of the Holocene terrace along the northeast side of the river. In this area the fault is characterized by a 500-m-long, N35°W-trending linear swale bounded on the southwest by a 2 to 4 meter high northeast facing scarp (Sites #146-149, Figure 6f). Impounded water along this scarp creates a long swampy bog. The linear valley extends to the mouth of Groshong Gulch, where the scarp decreases in size to about 1 meter.

At the mouth of the North Fork Gualala River, the fault traverses a Holocene fluvial terrace northeast of the river, and splits into two parallel fault splays. These two fault splays appear to offset a small stream ~3 m across each splay (Sites #150 and 151, Figure 6f). Directly north of the offset stream, the fault is characterized by a ~100-m-long, 2.5-m-high, northeast-facing scarp that bounds a swampy linear swale. Between this swampy swale and the mouth of the Little North Fork Gualala River (locally known as Elk Prairie), fault related geomorphology has been obscured by historic terrace sedimentation and historic logging operations (road building and log yarding). However, based on subtle linear swales, closed depressions supporting moisture dependent vegetation, and small (~1 m) scarps that traverse the outside

edge of the terrace deposits at meander bends in the river, the fault appears to closely follow the course of the North Fork Gualala River as a single trace (Table 3, Figure 6f and 6g). In the vicinity of Elk Prairie, long term tectonic control of the drainage pattern is evidenced by the northwest trend of the Little North Fork Gualala River and an abrupt bend to the northeast (perpendicular to the fault) of the North Fork Gualala River channel (Figure 5). At this location the fault trace is buried by historic flood deposits.

Table 3. Geomorphic features along the North Fork/Little North Fork Gualala River Section of the San Andreas fault (refer to Figures 6f to 6h)

Location	Geomorphic Feature	Site Number
Mouth of North Fork Gualala River to Elk Prairie	Linear swales and closed depressions	156, 157, 158, 159, 160, 161,
Elk Prairie to Log Cabin Creek	Southwest facing scarps and linear ridges and drainages	163, 164, 165, 167, 168, 169, 171, 172, 176, 177, 178, 180, 181, 182, 184, 190, 195, 197
Elk Prairie to Log Cabin Creek	Swampy linear swales, closed depressions, and ponds	163, 166, 170, 171, 177, 182, 193,
Elk Prairie to Log Cabin Creek	Right offset stream channels and beheaded streams	164, 169, 173, 175, 186, 188, 192, 196, 194, 199
Log Cabin Creek to Doty Creek	Southwest facing scarps and linear valleys	197, 200, 201, 202, 204, 205, 209, 213, 214, 216, 219, 220, 222, 223, 224
Log Cabin Creek to Doty Creek	Right offset stream channels and beheaded streams	210, 212, 215,
Doty Creek to drainage divide of Gualala Basin	Scarps and linear swales	226, 229, 231, 232, 236, 238, 239, 241, 242
Doty Creek to drainage divide of Gualala Basin	Offset stream channels and beheaded drainages	231, 234, 235, 237, 238,

Approximately 350 m north of the confluence, the fault projects from the Holocene terrace surface onto the lower part of the northeast facing slope that bounds the southwestern side of the Little North Fork Gualala river valley. In this area, the fault extends to the vicinity of Log Cabin Creek as a continuous single trace characterized by southwest facing scarps and linear ridges (~2-5 m high), swampy linear swales, and closed depressions (Table 3, Figures 6g and 6h). Major streams draining the northeast facing valley slope have been deflected southeast along the fault for various distances and create gaps in the southwest facing fault scarp. Smaller streams have ponded alluvium against the fault scarp and terminate in dry and swampy closed depressions. A tilted large old growth redwood tree (Figure 9) was observed at the base of the fault scarp at site #171. The base of the trunk of this tree is irregularly shaped and possibly was offset right laterally in the 1906 earthquake (Figure 9).

North of the vicinity of Log Cabin Creek, the fault continues along the southwestern valley slope of the Little North Fork Gualala River valley and is characterized by left stepping en echelon geometry that continues to the vicinity of Doty Creek (Figure 6h). Within the left stepping zone, individual fault traces range in length from about 500 to 1000 m and overlap and parallel adjacent traces by about 200 to 400 m (Figure 6h). Overlapping traces are characterized by parallel southwest facing scarps (2-3 m) and linear valleys that are approximately 30 to 50 m apart. Additional fault related geomorphology in these small

stepover zones include right laterally offset stream channels, abandoned stream channels that cut through scarps, sidehill benches, closed depressions, ponds, and ponded alluvium (Figure 6h, Table 3).

The fault becomes a single trace north of the vicinity of Doty Creek to the drainage divide with the Garcia River basin at the Mendocino County landfill facility. Along this reach of the fault, landslide processes and logging road construction have modified the topography, however, linear sidehill benches, a subtle linear valley, right offset stream channels, and a few short southwest facing scarps (2-4 m high) delineate the trace of the fault (Table 3, Figures 6h and 6i). The fault crosses the Little North Fork Gualala River and is expressed as a northeast facing scarp that traverses the southwest facing valley slope below the landfill, and extends to the western property boundary of the landfill. Adjacent to the western side of the landfill, the fault trace is delineated by a sidehill bench and a linear valley bounded by a northeast facing scarp.

Within the North Fork/Little North Fork Gualala River section, ponded alluvium occurs against scarps at sites #162, 172, 180, 181, 185, 187, 214. Of these sites only #172 and #214 are considered viable research sites and are discussed below in the section titled "Future Paleoseismic Research Site". The other sites are not considered viable for the following reasons. Site #162 has coarse gravel colluvium deposited against the fault, lacks fine grained alluvium, and is heavily vegetated with underbrush and softwood trees. At sites #180 and #181, the fault location is constrained by a linear valley and right-laterally offset stream, however there is no accessible approach for equipment to get through the thick vegetation and over the steep road-cut and southwest facing scarp from the nearest logging road located approximately 30 m to the east of the site. At sites #185 and #187, the fault projects across an alluvial flat where the scarp is buried by fine grained alluvial material sourced from a small stream to the west. Unfortunately, this site has experienced a heavy amount of historic modification due to previous logging operations and much of the alluvium may be historic in age.

4.2.3 Garcia River Section

The Garcia River section extends from the drainage divide between the Garcia and Gualala River basins to Point Arena (Figure 5 and Figures 6i and 6j). For this study, however, we only characterize the fault from the drainage divide to Voorhees Grove (~1 km north of the confluence between the Garcia River and South Fork Garcia River). In general, the fault trace extends west of and parallel to the channels of the South Fork Garcia River and Garcia River. Navigating and mapping in this section is much more difficult than areas to the south due to debris left by past logging operations (Figure 10). In following the fault, we were forced to traverse through thick dead sticks and branches and sometimes had to crawl on the ground. The LIDAR data proved invaluable for field locating and navigation in these regions of dense vegetation. Because points of reference (i.e., roads, creek names) are virtually non-existent along the fault in this section, we describe the fault in relation to a large shutter ridge that extends south from the South Fork/Main stem Garcia Rivers confluence along the south-western side of the South Fork Garcia River channel for about 1.8 kilometers (Figure 5, labeled "shutter ridge"). This shutter ridge is a prominent feature along the fault and is easily recognized on both the LIDAR data and USGS 7.5 minute Gualala, California quadrangle (Figures 6i and 6j).

North of the drainage divide to the southern side of the large shutter ridge, the fault is characterized by two parallel traces separated by approximately 125 m (Figure 6i). The eastern trace extends about 500 m north from the drainage divide and is characterized by a long linear valley, closed swampy depressions, and a southwest facing scarp that ranges in height from 2-5 m (Table 4). The scarp diminishes in height to the north and projects to a sidehill bench that marks the northernmost 100 m of the strand. The western trace extends north from the drainage divide and is characterized by a large (~5 m) southwest facing scarp and continuous linear valley that contains ponded water for about 500 m (Table 4). This trace appears to splay into three parallel traces that are continuous for approximately 450 m and located directly south of

the large shutter ridge (Figures 5, 6i, and 7). The westernmost splay is characterized by a long linear stream valley, a large pond, southwest facing scarp, and ponded alluvium against the scarp. This splay terminates at a large inner gorge landslide, but appears to project towards the southwestern side of the shutter ridge to the north. The eastern splay is characterized by a northeast facing sidehill bench and linear valley. Evidence of this splay has been removed in the stream valley to the north and we were unable to determine whether the splay continues to the north where it projects onto the shutter ridge. The middle splay is characterized by a linear valley and southwest facing scarp (N25°W). This splay projects across the creek valley and follows a subtle linear valley uphill along the southwest facing wooded slope of the shutter ridge for about 250 m.

This sub-section of the fault (drainage divide to southern side of shutter ridge) represents the most complex fault geometry encountered during our mapping. In contrast to areas to the north and south of this sub section, the fault in this location has a much broader zone of deformation (~150 m) distributed across three main splays that appear to accommodate a left step as the fault changes orientation from about N25°W to N34°W (Figure 7). To the south, en echelon steps in the fault trace are typically less than about 40 m and to the north the fault extends mostly as a single fault trace. This complex geometry may indicate a potential rupture segment boundary. However, paleoseismic investigations along the fault north and south of this stepover zone are necessary to confirm this hypothesis.

Beginning at the southern side of the shutter ridge, the fault becomes primarily a single trace that extends north to the vicinity of Voorhees Grove (map area boundary) (Figures 6i and 6j). The fault defines the southwestern edge of the shutter ridge and trends parallel to (~30 m west) and overlaps the middle splay described above by about 200 m. In this area the fault is characterized by a long narrow linear valley that ranges in width from about 5 to 15 m. Ephemeral streams within the linear valley alternate between southeast flowing and northwest flowing. Large ponds up to 250 m long fill the linear valley (Table 4). At the northwestern side of the shutter ridge the fault follows an approximately 300 meter long linear valley that trends along the northeastern slope of a northwest trending linear stream valley. To the north of this stream valley, the fault projects into a large deep seated landslide complex (Site #300, Figure 6j) where geomorphic evidence of the fault location has been obscured. North of the landslide complex, the fault is characterized by a N40°W-trending southwest facing scarp, large pond, and linear valley that extends to a south-facing bedrock cliff on the margin of a large tributary creek. Bedrock exposed in the wall consists of Tertiary rocks west of the fault and pulverized Franciscan Formation east of the fault. We were unable to locate the fault for a short distance north of the bedrock exposure, however, we infer that the fault steps ~30 m to the east and extends across the inner gorge landslide slope that lies along trend of the fault between sites #303 and #304 (Figure 6j).

North of site #304, the fault is characterized by a sidehill bench, southwest facing scarp (2-3 m high), linear valley, multiple ponds, and right-laterally offset ephemeral stream channels (Table 4). The orientation of the fault in this area changes at a small left step (~30m) from N20°W to N35°W. A short strand approximately 100 m east of the main fault trace is associated with a narrow linear valley (~5 m) and a ~1.5-m-high southwest facing scarp.

We observed alluvium ponded against the fault within narrow linear valleys throughout the Garcia River section. Paleoseismic research at most of these localities is not possible due to access limitations caused by the large amounts of logging debris and limited road maintenance. Although access would be difficult, site #271, directly south of the large shutter ridge, contains favorable sediments for paleoseismic research. The fault is relatively well defined by a southwest facing scarp. The scarp projects into an alluvial flat where a few streams come together near a linear swale. The combination of stream deposition and intermittent pond deposition against the scarp is favorable for preserving a record of event timing. Accessing this site would require approximately 200 m of brush and small tree removal along an old logging road.

Table 4. Geomorphic Features along the Garcia River Section of the San Andreas fault (refer to Figures 6i and 6j)

Location	Geomorphic Feature	Site Number
Drainage divide to south side of shutter ridge	Scarps and linear valleys/drainages	245, 247, 251, 253, 254, 255, 252, 256, 257, 259, 260, 262, 263, 267, 269, 270, 273, 275, 276, 278
Drainage divide to south side of shutter ridge	Ponds and swampy depressions	245, 246, 248, 250, 252, 254, 256, 257, 259, 260, 273, 278, 279, 280
Shutter ridge to Voorhees Grove	Scarp and linear valleys/drainages	282, 283, 288, 289, 290, 292, 293, 295, 296, 297, 298, 299, 301, 303, 306, 308, 309, 311, 312, 313, 314, 315, 316, 317, 318, 319
Shutter ridge to Voorhees Grove	Ponds and swampy depressions	280, 285, 287, 288, 294, 299, 301, 302, 306, 309, 311
Shutter ridge to Voorhees Grove	Offset stream and beheaded channels	291, 307, 316

4.3 Future Paleoseismic Research Site

A fundamental question that should be addressed by future research along the northern San Andreas fault is whether or not there are differences in slip rate and recurrence rate in the Gualala area comparable/similar to paleoseismic data to the north (Point Arena) and south (Fort Ross) (Figure 1). This question is critical to evaluating whether the fault characteristically ruptures in similar-sized 1906 type ruptures or ruptures on discrete, smaller fault segments (i.e. North Coast segment; WGCEP, 2003). Earthquake recurrence and timing information from multiple sites along the fault are necessary to evaluate the merits of these contrasting models. Additionally, on-land data is necessary to validate offshore turbidite event chronologies being developed by Goldfinger et al. (2003). Currently, no paleoseismic data exists within the Gualala River Valley, however we identify two possible research sites to test these rupture models.

In the Little North Fork Gualala River valley approximately 1500 m northwest of the confluence between the Little North Fork and North Fork Gualala Rivers the fault is expressed as a single trace (Figure 6g). Along this stretch of the fault we have identified a potential paleoseismic research site (Site #172, Figure 6g). This site is a favorable for future paleoseismic trench study because: (1) the fault appears to be a single trace and would presumably record the total amount of deformation; (2) youthful geomorphic features, including a ~2.5 meter-high southwest facing scarp, a right laterally offset stream directly north of the site, and a linear valley and pond directly south of the site clearly delineate the fault location; (3) Holocene alluvium sourced from a small stream valley abuts the scarp providing favorable stratigraphy for determining event chronology; and (4) an old logging road extends a short distance from the Little North Fork Road providing good access to the site. This access location is adjacent to culvert number 60 installed across the Little North Fork Road by Gualala Redwood Company in 2003.

Approximately 300 m south of the mouth of Doty Creek, we identified an alternative research site that may also be favorable for paleoseismic research (Site #214, Figure 6h). At this site the fault is well defined by a southwest facing scarp (~2 m high) that has deflected a small stream. North of this point of deflection the scarp diminishes in height and is buried by fine grained alluvium. An old logging road can be used to access the site, however alder trees growing in the road bed would have to be cleared to provide access for equipment.

Although we identified multiple sites where paleoseismic trenching would possibly generate quality event timing and recurrence information, the sites described above have the best access for heavy equipment necessary for trenching and are not as heavily vegetated as other potential sites. Access to other sites is severely limited due to the rugged topography, dense vegetation and logging debris. Therefore, we suggest that future paleoseismic efforts should be focused to develop data at site #172 or possibly site #214.

5.0 DISCUSSION AND CONCLUSION

The map presented here represents a significant refinement of the location of active fault strands of the northern San Andreas fault and improves upon the previous mapping of Brown and Wolfe (1972), which relied primarily on the interpretation of aerial photographs and limited field reconnaissance. These field based maps will ultimately be incorporated into a larger study being conducted by Dr. Carol Prentice (USGS) aimed at remapping the entire 70-km-long on-land part of the northern San Andreas fault using LIDAR data. The final USGS map product will be a digital GIS-based strip map of the northern San Andreas fault between Fort Ross and Point Arena.

For this study, the LIDAR data proved to be an invaluable tool for mapping the location of active fault strands and tectonic related geomorphology. However, office-based LIDAR interpretation must be combined with field reconnaissance because of inconsistencies in interpretation and LIDAR data quality. We found that some lineaments identified as faults from the on-screen images were determined in the field to be old logging roads, power lines, or other features unrelated to faulting. For most of the 24-km long study area, the LIDAR images were clear and provided superior resolution to traditional base maps. In a few areas, the LIDAR was of poor quality either because the vegetation was too dense or the data was acquired with poor laser ground returns. In these areas, topographic maps and aerial photographs were helpful. Also, comparison with earlier mapping of the northern San Andreas fault (Brown and Wolfe, 1972) shows that in some areas the LIDAR data allow a correction of the fault trace location of up to several hundred meters. The combined approach of on-screen mapping and field reconnaissance, shows the effectiveness of using LIDAR to produce accurate and detailed maps of fault traces and fault related features.

Despite the effects of heavy rainfall, bioturbation, and cultural modifications (i.e. logging) along the mapped stretch of the San Andreas fault, differentiating the 1906 rupture trace is possible in some areas through careful field observations and mapping. In areas where the fault is a single trace, the 1906 rupture scarp is often recognizable as a distinct ~1-2 m high southwest facing scarp coincident with other fault controlled geomorphic features. For example, in the Gualala River Section, we infer that the 1906 rupture trace follows the singular fault trace between sites # 31-35 where the scarp is coincident with long narrow ponds and beheaded stream channels and between sites #78-96 where it is coincident with a linear valley, offset streams, and ponds. At the northern end of the Gualala River Section, we are less confident in the exact location of the 1906 rupture trace due to more subtle geomorphic expression, as well as partial removal of fault geomorphology by bank erosion of the Gualala River. We infer that the 1906 rupture trace is well defined in the North Fork/Little North Fork Gualala River Section, by a singular trace expressed as a prominent southwest facing scarp associated with a linear valley, beheaded streams, swampy depressions, and ponds (Sites #162-177, Figure 6g). At the northern end of the Garcia River Section, we further infer that the 1906 rupture trace is associated with a single southwest facing scarp coincident with pirated channels, youthful looking stream offsets, and a narrow linear valley (Sites #309, 310, 314-319, Figure 6j). We attribute the preservation of the 1906 rupture trace in this area to the location of the trace on a hillside with little ponding and sedimentation, as well as minimal cultural disturbance due to the steep terrain.

In areas with long parallel traces or multiple stepping traces, the 1906 rupture is more difficult to recognize, and we often were unable to differentiate between the 1906 rupture trace and other previous ruptures. For example, in the Gualala River Section, parallel southwest facing scarps exhibit similar morphology and size and are often partially buried by pond sediments (Sites #28, 29, and 30, Figure 6b; Sites #42-52, Figure 6b; Sites #68-75, Figure 6c). These scarps commonly bound parallel linear valleys and represent landscape development over many seismic cycles. Although we are not confident of the exact location of the 1906 rupture trace in these areas, we infer that it is close to and probably within ~10 m of the mapped trace within the longer or more prominent of two parallel linear valleys. In contrast to

the Gualala River Section (parallel stepping traces), the northern part of the North Fork/Little North Fork Gualala River Section (north of site #74, Figure 6g and 6h) is characterized by stepping traces that only overlap for short distances. We infer that the 1906 rupture trace is well located along individual traces in this area, generally associated with southwest facing scarps, linear valleys, and offset and beheaded streams. However, in the stepover areas, the exact location of the 1906 rupture is not well constrained due to subtle geomorphic expression and heavy vegetation. Prominent left stepping parallel traces characterize the fault along the southern part of the Garcia River Section. We infer that the 1906 rupture trace follows the eastern trace at the drainage divide and steps over to the western trace (Sites #243-260, figure 6i). Between sites #261 and #276, we were unable to differentiate the trace of the 1906 rupture due to similar geomorphic expression and size of each scarp bounding the stepping traces. North of site #276, we infer that the 1906 rupture trace returns to a well constrained singular trace and closely follows the prominent linear valley along the west side of the shutter ridge (Figures 5, 6i, and 6j).

Comparison of our LIDAR and field mapping to previous maps (Brown and Wolf, 1972) indicates that the LIDAR allows a more detailed depiction of active fault traces and that the fault trace geometry is more complex than originally shown on the 1972 maps. Overall, the fault maintains a consistent N35°W-N45°W orientation within the mapped region, however, our mapping identified two zones of complexity that may represent segment boundaries. Based on the expression of the fault as a singular trace north and south of a right stepping zone of short faults at the northern end of the Gualala River Section, we infer that this zone is more likely related to a subtle change in fault orientation and not representative of a rupture segment boundary. The most complex zone of stepping splays occurs in the area of the drainage divide between the Gualala and Garcia River valleys along the southern end of the Garcia River Section of the fault (Figures 6i and 7). North and south of this area the fault extends as a single trace. Based on the presence of river gravel deposits in the drainage divide, the left-stepping geometry of the fault traces has provided a restraining geometry in a right lateral system that has caused uplift and abandonment of a former river valley. We infer that the major change in the expression of the fault, the fault trace complexity, and the width of the stepovers between individual traces may indicate that a fault rupture segment boundary may exist at the drainage divide. This inferred rupture segment boundary did not appear to arrest the rupture in 1906. Therefore, development of paleoseismic data at sites north and south of the drainage divide are necessary to evaluate whether previous ruptures have always propagated through this complex zone or if it represents a rupture segment boundary for smaller ruptures.

Whether or not the northern San Andreas fault has asperities or rupture segment boundaries remains a critical question to seismic hazards assessment for the greater San Francisco Bay Area and north coast regions. Potential segmentation boundaries along the northern San Andreas fault have implications to the size of future earthquakes on the fault. Therefore, detailed mapping, as performed in this investigation, coupled with future paleoseismic investigations are essential elements of seismic hazards assessment. We emphasize that the length of the fault encompassed in this mapping project may be too short to recognize major regional fault segment boundaries. A more regional detailed map of the entire fault trace from Fort Ross to Point Arena (presently being compiled by Dr. Prentice), combined with paleoseismic investigations at multiple sites along the fault is necessary to ultimately determine whether or not segment boundaries exist along the northern San Andreas fault. Paleoseismic research sites defined in this project provide an initial first step towards understanding the rupture behavior of the San Andreas fault in the Gualala River valley.

6.0 ACKNOWLEDGMENTS

This project was funded by the U.S. Geological Survey's National Earthquake Hazards Reduction Program (Award # 03HQGR0045). We would like to acknowledge Henry Alden (Gualala Redwoods Company) and Chris Surfleet (Mendocino Redwoods Company) for graciously allowing us access to their property to conduct field mapping. We are grateful for assistance in the field from Ryan Crawford (Humboldt State University) and Julie Bawcom (California Geological Survey). Andrew Barron (University of Nevada, Reno), Jason Holmberg and Carolyn Mosher (William Lettis & Associates, Inc.) assisted with preparing and drafting the figures.

7.0 REFERENCES

- Baldwin, J.N., 1996, Paleoseismic investigation of the San Andreas fault on the north coast segment, near Manchester, California: M.S. thesis San Jose State University, 127, p. plus plates.
- Baldwin, J.N., Knudsen, K.L., Lee, A., Prentice, C.S. and Gross, R., 2000, Preliminary estimate of coseismic displacement of the penultimate earthquake on the northern San Andreas fault, Pt. Arena, California, *in* Proceedings of the 3rd conference on Tectonic Problems of the San Andreas Fault System, Bokelmann, G. and Kovach, R.L. *eds*, Stanford University, Stanford, California.
- Best, T., 1997, Gualala River Watershed Analysis, Unpublished Technical Report to Gualala Redwood Company.
- Brown, R.D., and Wolfe, E.W., 1972, Map showing recently active breaks along the San Andreas Fault Between Point Delgada and Bolinas Bay, California: U.S. Geological Survey, Miscellaneous Geologic Investigations, Map 1-692.
- California Geological Survey (CGS), 2003, Reproduced with permission, California Geological Survey CD-ROM 2002-08, Watershed Mapping Series, Map Set 5, Gualala River Watershed, Sonoma and Mendocino Counties.
- Fumal, T.E., Dawson, T.E., Flowers, R., Hamilton, J.C., Kessler, J., and Samrad, L., 2004, A 100-yr average recurrence interval for the San Andreas fault, southern San Francisco Bay area, California [abs.]: First Annual Northern California Earthquake Hazards Workshop, U.S. Geological Survey, Menlo Park, January 13, 2004, p. 42.
- Goldfinger, C. and Nelson, C.H., 2000, Holocene Seismicity of the Northern San Andreas Fault Based on the Turbidite event record, *in* Proceedings of the 3rd conference on Tectonic Problems of the San Andreas Fault System, Bokelmann, G. and Kovach, R.L. *eds*, Stanford University, Stanford, California.
- Goldfinger, C., Nelson, C.H., and Johnson, J.E., 2001, Temporal Patterns of turbidites offshore the Northern San Andreas Fault and Correlation to Paleoseismic events onshore, *Eos Transactions AGU*, 82(47) Fall Meeting Supplement, Abstract S52D-0672.
- Goldfinger, C., Nelson, C.H., Johnson, J.E., and The Shipboard Scientific Party, 2003a, Holocene earthquake records from the Cascadia subduction zone and northern San Andreas fault based on precise dating of offshore turbidites: *Annual Reviews of Earth and Planetary Science*, v. 31, pp. 555-577.
- Hall, N.T., Wright, R.H., and Clahan, K.B., 1999, Paleoseismic studies of the San Francisco Peninsula segment of the San Andreas fault zone near Woodside, California: *Journal of Geophysical Research*, v. 104, no. B10, p. 23,215-23,236.
- Haugerud, R.A., Weaver, C.S., and Harless, J., 2001, Finding Faults with LIDAR in the Puget Lowland: *Seismological Research Letters*, v. 72, p.253.
- Hill, D.P., Eaton, J.P., and Jones, L.M., 1990, Seismicity, 1980-1986, in Wallace, R.E., ed., the San Andreas fault System California: U.S. Geological Survey Professional Paper 1515, p. 115-151.

- Johnson, S.Y., A.R. Nelson, S.F. Personius, R.E. Wells, H.M. Kelsey, B.L. Sherrod, K. Okumura, R. Koehler, III, R. Witter, L. Bradley, and D.J. Harding, 2004, Evidence for late Holocene earthquakes on the Utsalady Point fault, northern Puget Lowland, Washington: Bulletin of the Seismological Society of America, v. 94, no. 6.
- Kelson, K.I., Koehler, R.D., and Kang, K.-H., 2003, Initial evaluation of paleoearthquake timing on the northern San Andreas fault at the Fort Ross Orchard site, Sonoma County, California: Final Technical Report submitted to the U.S. Geological Survey National Earthquake Hazard Reduction Program, Award No. 00HQGR0072, 29 p.
- Kelson, K.I., Streig, A., and Koehler, R.D., 2005, Preliminary Evaluation of Paleoseismicity Timing, northern San Andreas Fault, Fort Ross, CA [abs.] : Geological Society of America Abstracts with Programs, v. 37, no. 4; San Jose, California.
- Knudsen, K.L., Witter, R.C., Garrison-Laney, C.E., Baldwin, J.N., and Carver, G.A., 2002, Past Earthquake-Induced Rapid Subsidence along the Northern San Andreas Fault: A Paleoseismological Method for Investigating Strike-Slip Faults, Bulletin of the Seismological Society of America, v. 92, no. 7, pp. 2612-2636.
- Lawson, A.C., chairman, 1908, the California earthquake of April 18, 1906: Report of the State Earthquake Investigation Commission (Reprinted 1969), v. 1, Carnegie Institution of Washington Publication, 451 p. and atlas.
- Loomis, K.B., and Ingle, J.C., Jr., 1994, Subsidence and uplift of the Late Cretaceous-Cenozoic margin of California: New evidence from the Gualala and Point Arena basins: Geological Society of America Bulletin, v. 106, p. 915-931.
- Nelson, A.R., Johnson S.Y., Kelsey, H.M., Wells, R.E., Sherrod, B.L., Pezzopane, S.K., Bradley, L.A., Koehler, R.D., and Bucknam, R.C., 2003, Late Holocene Earthquakes on the Toe Jam Hill Fault, Seattle Fault Zone, Bainbridge Island, Washington: Geological Society of America Bulletin, v. 115, no. 11, p. 1388-1403.
- Niemi, T.M., 2002, Determination of a high resolution paleoearthquake chronology for the northern San Andreas fault at the Vedanta marsh site, Marin County, CA: U.S. Geological Survey, National Earthquake Hazard Reduction Program, Final Technical Report, Award # 01HQGR0194.
- Niemi, T.M. and Hall, N.T., 1992, Late holocene slip rate and recurrence of great earthquakes on the San Andreas fault in northern California: Geology, v. 20, p. 195-198.
- Niemi, T.M., Zhang, H., Generaux, S., Fumal, T. and Seitz, G., 2002, A 2500-year record of earthquakes along the northern San Andreas fault at Vedanta Marsh, Olema, CA [abs]: Geological Society of America Cordilleran Section, 98th Annual Meeting Abstracts with Programs, v. 34, no. 5, p. 86.
- Noller, J.S., and Lightfoot, K.G., 1997, an archaeoseismic approach and method for the study of active strike-slip faults: Geoarchaeology: An International Journal, v. 12, p. 117-135.
- Noller, J.S., Kelson, K.I., Lettis, W.R., Wickens, D.A., Simpson, G.D., Lightfoot, K., Wake, T., 1993, Preliminary characterizations of Holocene activity on the San Andreas fault based on offset archaeological sites, Fort Ross State Historic park, California: U.S. Geological Survey, National Earthquake Hazards Reduction Program, Final Technical Report.

- Prentice, C.S., 1989, Earthquake geology of the northern San Andreas fault near Point Arena, California: California Institute of Technology, Pasadena, California, PhD Dissertation, 252p.
- Prentice, C.S., Merritts, d.J., Beutner, E.C., Bodin, P., Schill, A., and Muller, J.R., 1999, Northern San Andreas fault near Shelter Cove, California: Geological Society of America Bulletin, v. 111, no. 4, p. 512-523.
- Prentice, C.S., Langridge, R., and Merritts, D.J., 2000, Paleoseismic and Quaternary tectonic studies of the San Andreas fault from Shelter Cove to Fort Ross: *in* Bokelman, G., and Kovachs, R. (eds.), Tectonic problems of the San Andreas fault system, Stanford University Publications, p. 349-351.
- Prentice, C.S., Prescott, W.H., and Langridge, R., 2001, New geologic and geodetic slip rate estimates on the North Coast San Andreas fault: Approaching agreement? [abs]: Seismological Research Letters, v. 72, no. 2, p. 282.
- Schwartz, D.P., Pantosti, D., Okumura, K., Powers, T.J., and Hamilton, J.C., 1998, Paleoseismic investigations in the Santa Cruz Mountains, California: Implications for recurrence of large-magnitude earthquakes on the San Andreas fault: Journal of Geophysical Research, v. 103, p. 17,985-18,001.
- Simpson, G.D., Noller, J.S., Kelson, K.I., and Lettis, W.R., 1996, Logs of trenches across the San Andreas fault, Archae Camp, Fort Ross State Historic Park, Northern California: U.S. Geological Survey, National Earthquake Hazards Reduction Program, Final Technical Report.
- Spittler, T., 1982, Geomorphic Features related to landsliding, Gualala 7.5 minute quadrangle, California Division of Mines and Geology, watershed map series.
- Surfleet, C., and Koehler, R.D., 1998, Garcia River Watershed Analysis, Unpublished Technical Report to Louisiana-Pacific Corporation, pp. 160.
- Thatcher, W., Marshall, G., and Lisowski, M., 1997, resolution of fault slip along the 470-km-long rupture of the great 1906 San Francisco earthquake and its implications: Journal of Geophysical Research, v. 102, no. B3, p. 5353-5367.
- Varnes, D.J., 1958, Landslide types and processes, Highway Research Board, Special Report, 29: 20-47, Washington D.C.
- Wallace, R.E., ed., 1990, The San Andreas Fault System, California: U.S. Geological Survey Professional Paper 1515, United States Printing Office, Washington.
- Wentworth, C.M., Jr., 1966, The Upper Cretaceous and Lower Tertiary rocks of the Gualala area, northern Coast Ranges, California: unpublished Ph.D. thesis, Stanford University, figure 3, scale 1:62,500.
- Working Group on California Earthquake Probabilities (WGCEP), 1990, Probabilities of large earthquakes in the San Francisco Bay region, California: U.S. Geological Survey Circ. 1053, 51 p.
- Working Group on California Earthquake Probabilities (WGCEP), 2003, Earthquake probabilities in the San Francisco Bay Region: 2002-2031: U.S. Geological Survey, Open File Report 03-214.

Zhang, H., 2005 (in preparation), Paleoseismic studies of the northern San Andreas fault at Vedanta Marsh site, Olema, California: Ph.D. Dissertation, University of Missouri-Kansas City.

FIGURES

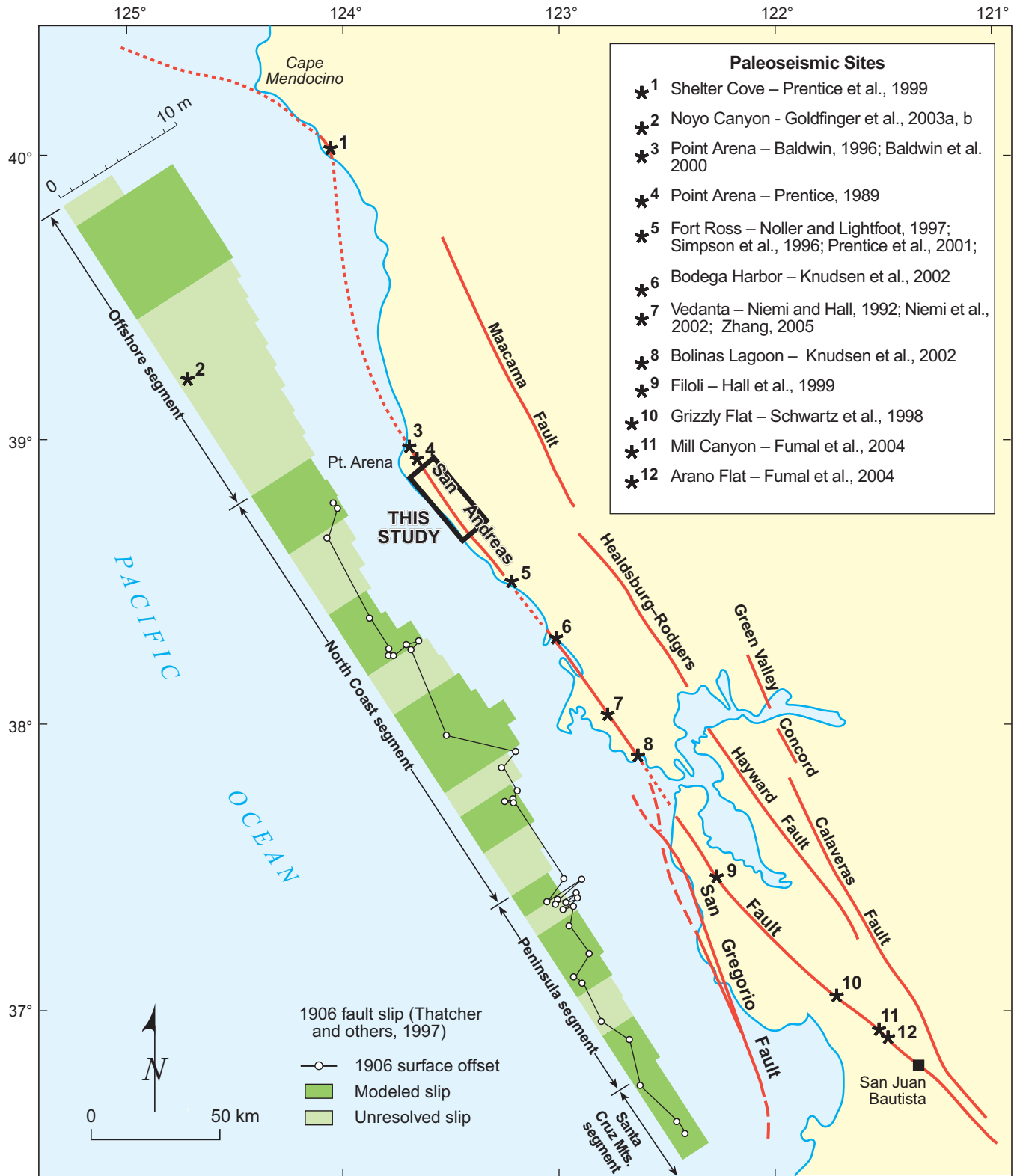


Figure 1. Regional map of the San Andreas fault in northern California, showing location of 1906 rupture, the North Coast segment of the fault, previous paleoseismic sites along the fault, distribution of surface geodetic slip produced by the 1906 rupture, (Thatcher, et al., 1997), and approximate location of the map area.

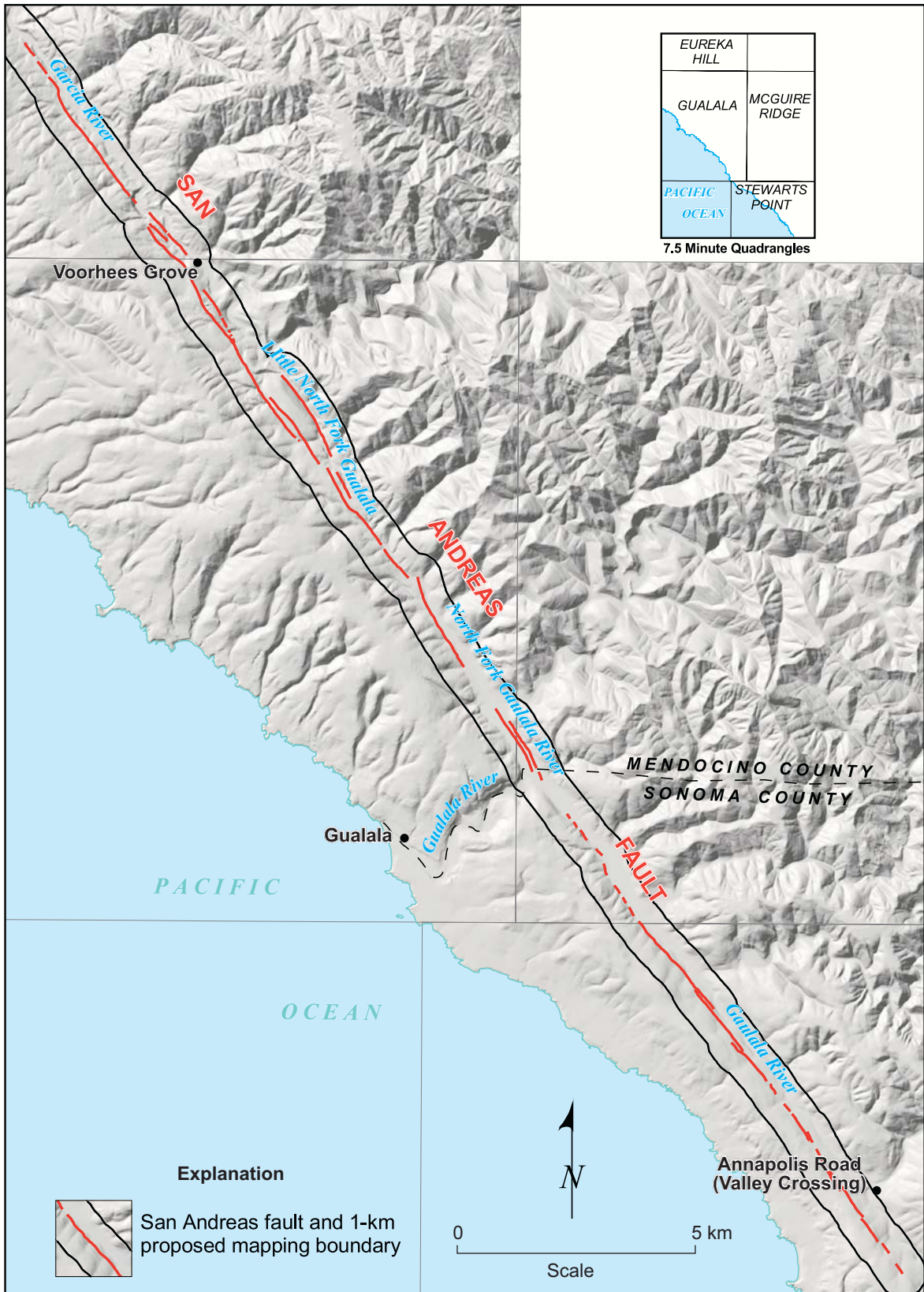


Figure 2. Shaded relief map of the North Coast segment of the San Andreas fault between Valley Crossing in the Gualala River Valley and Voorhees Grove in the Garcia River Valley. Generalized faults from Brown and Wolfe (1972) shown within our 1-km wide mapping boundary. (Map compiled by Andrew Barron, University of Nevada, Reno.)

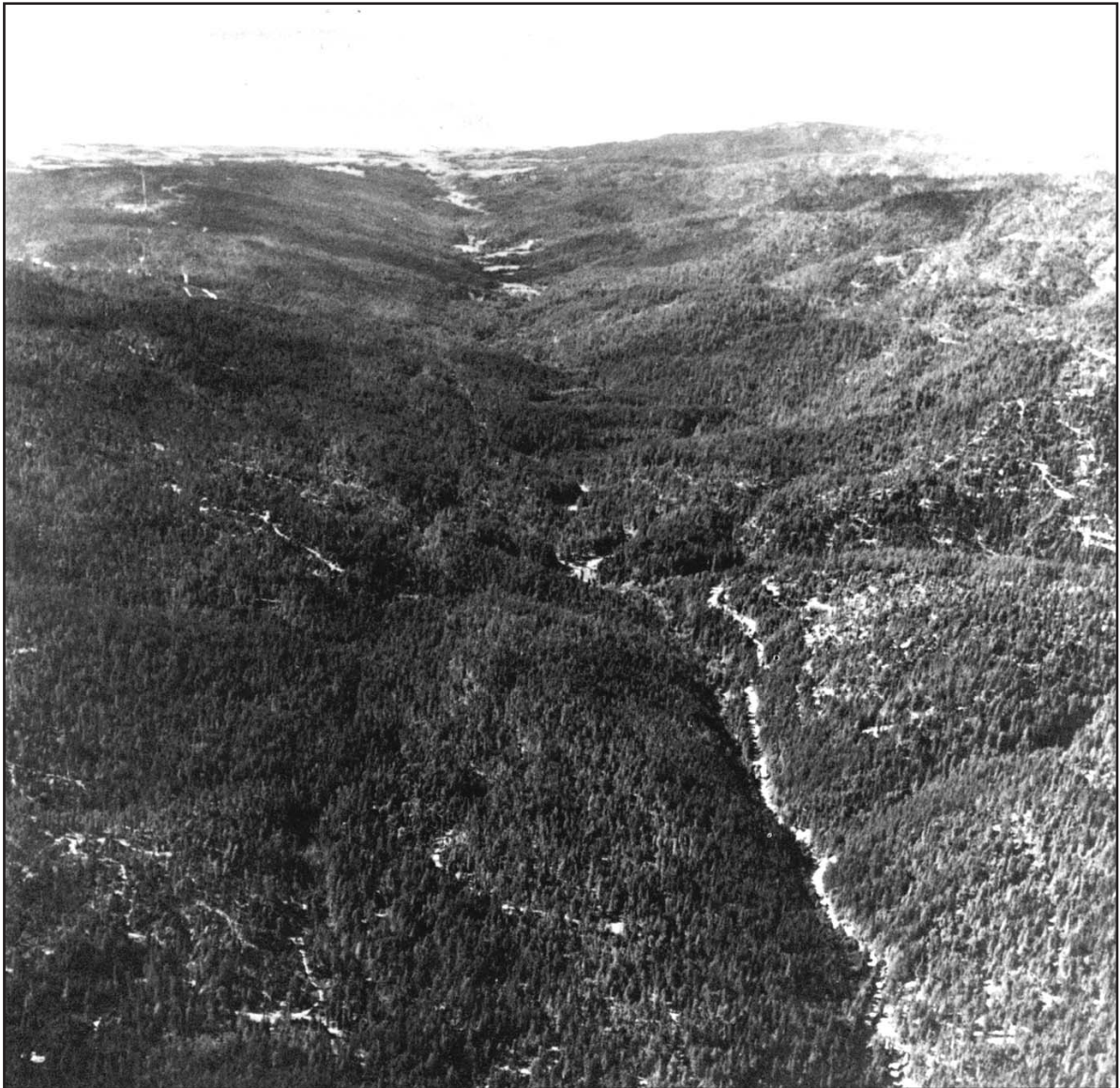
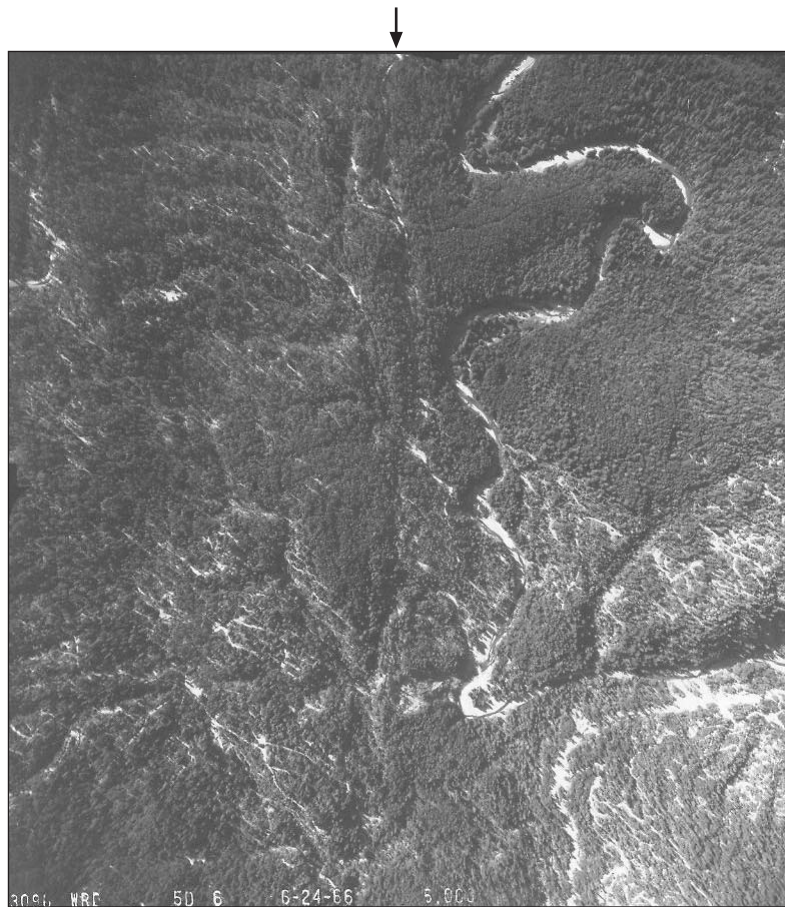
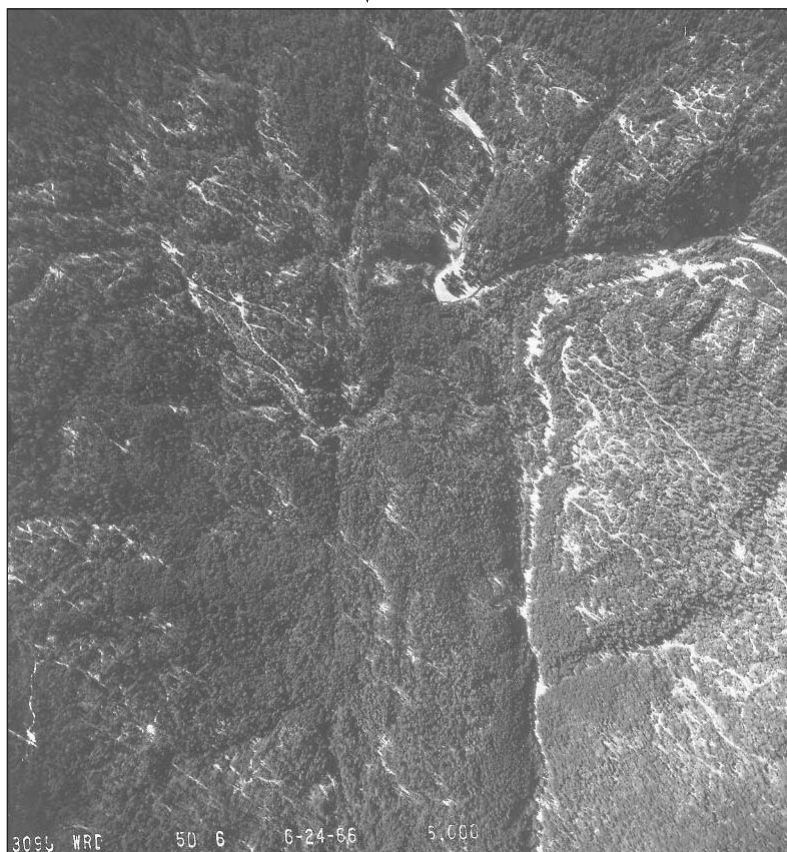


Figure 3. Northwest view from the vicinity of Fish Rock Road of the San Andreas fault in the Garcia River Valley. Splays of the fault bound the large shutter ridge in the middle foreground. The dense forest overstory makes the use of air photos in delineating fault related features difficult. The use of LIDAR Imagery in this project eliminates the vegetative cover and allows detailed interpretation of fault-related geomorphology. Photo from (Wallace, 1990).



San Andreas fault



San Andreas fault

Figure 4. Circa 1966 aerial photographs of the Garcia River Valley showing dense vegetation and heavy modification by past logging operations along the northern San Andreas fault. Black arrows indicate approximate location of the fault zone.



Figure 5. Location map showing distribution of major drainages and place names along the northern San Andreas fault within the study area as described in the text. Also shown are the boundaries of geomorphic description sections. Streams are generally parallel to the northwest-trending fault rift valley or perpendicular to the fault.

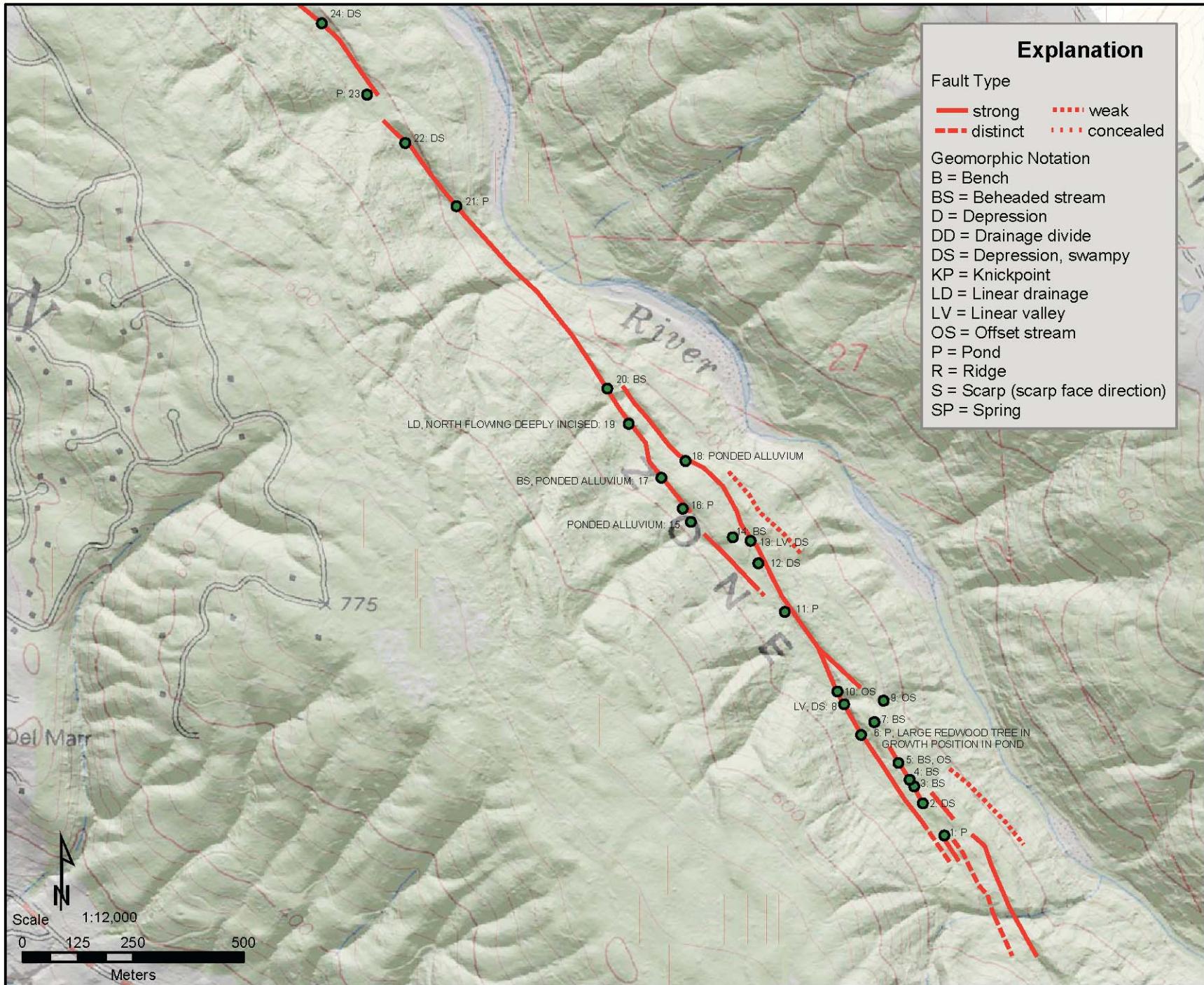


Figure 6a. Gualala River section of the San Andreas Fault. See Figure 7 for general location.

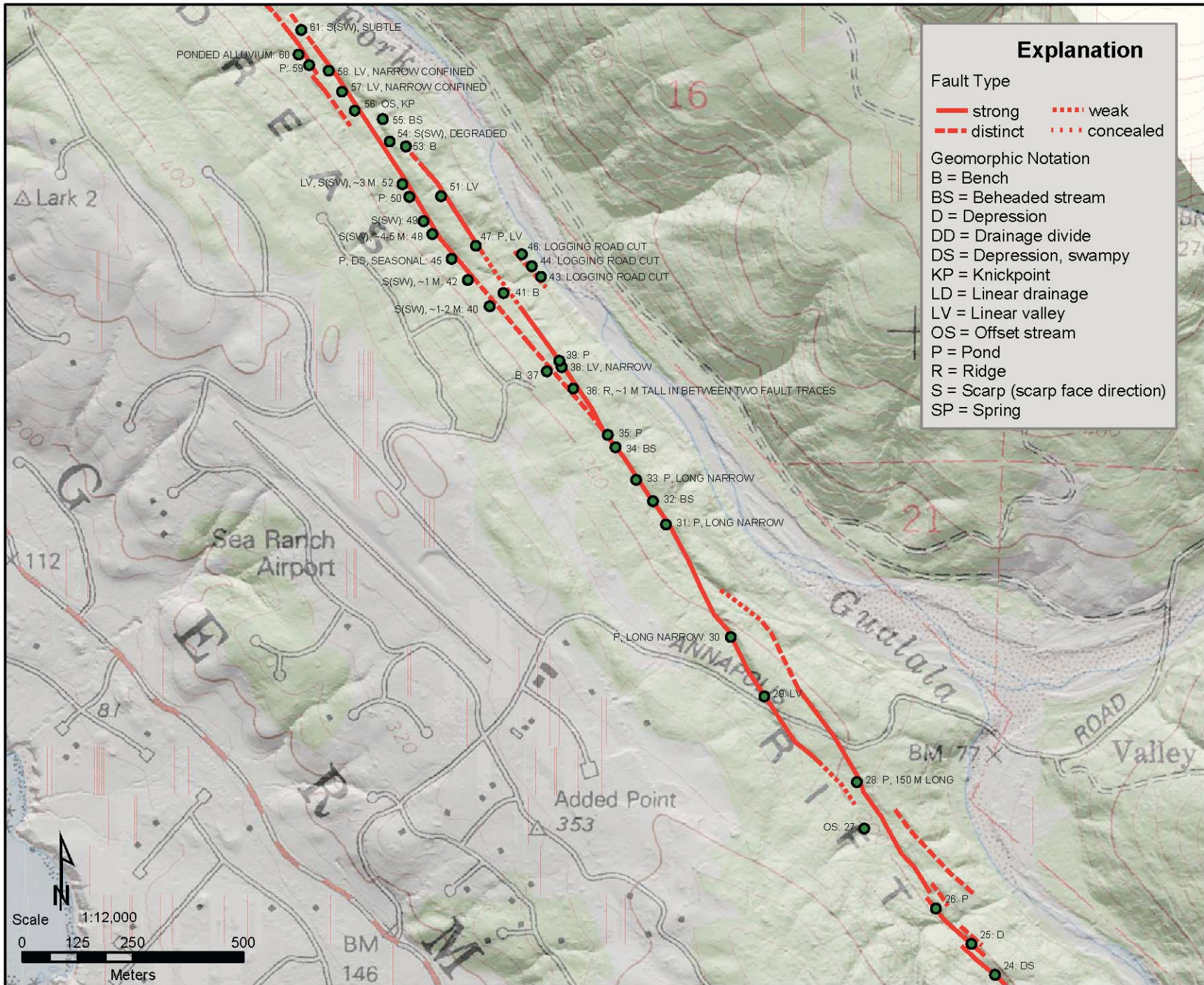


Figure 6b. Gualala River section of the San Andreas Fault. See Figure 7 for general location.

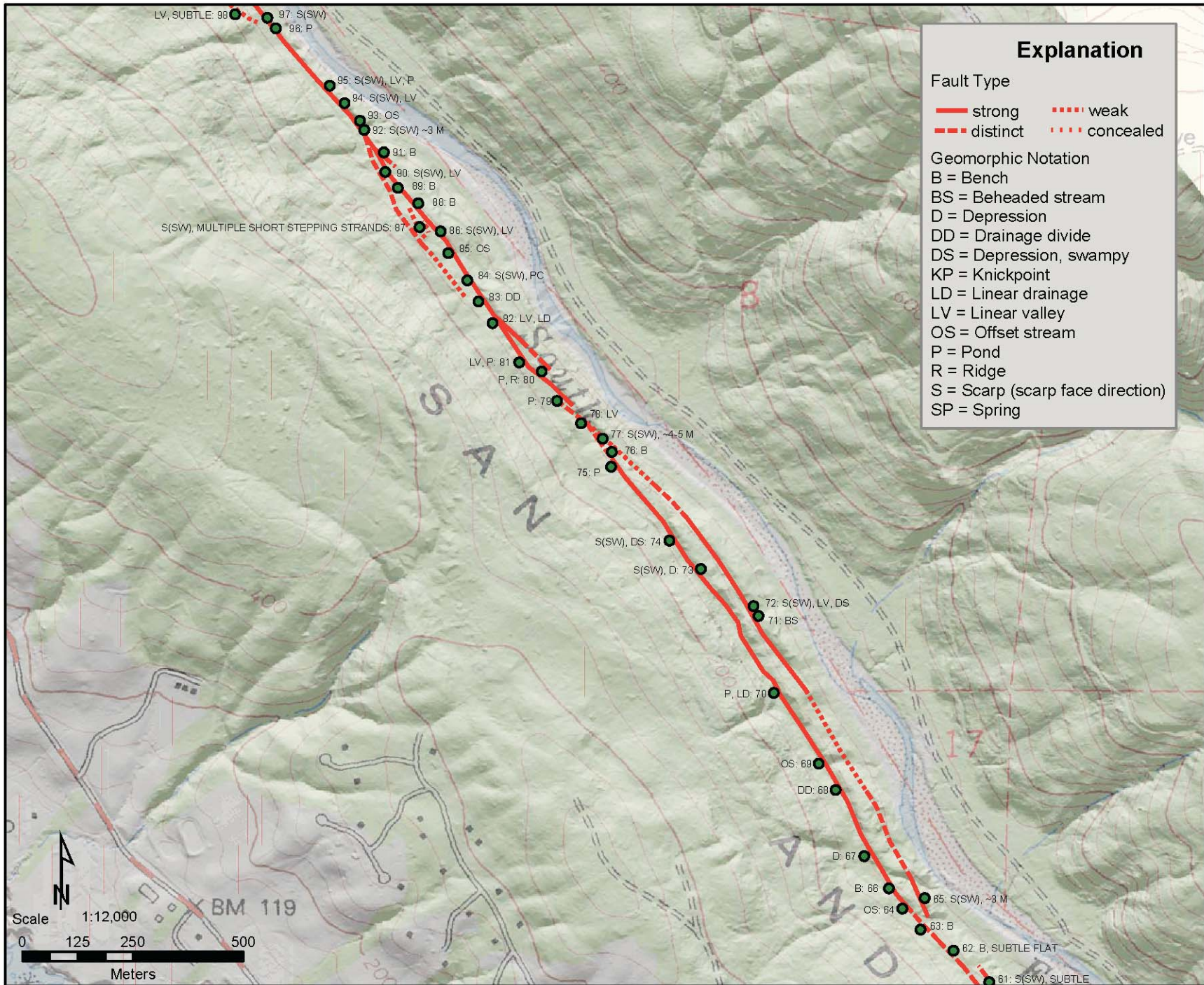


Figure 6c. Gualala River section of the San Andreas Fault. See Figure 7 for general location.

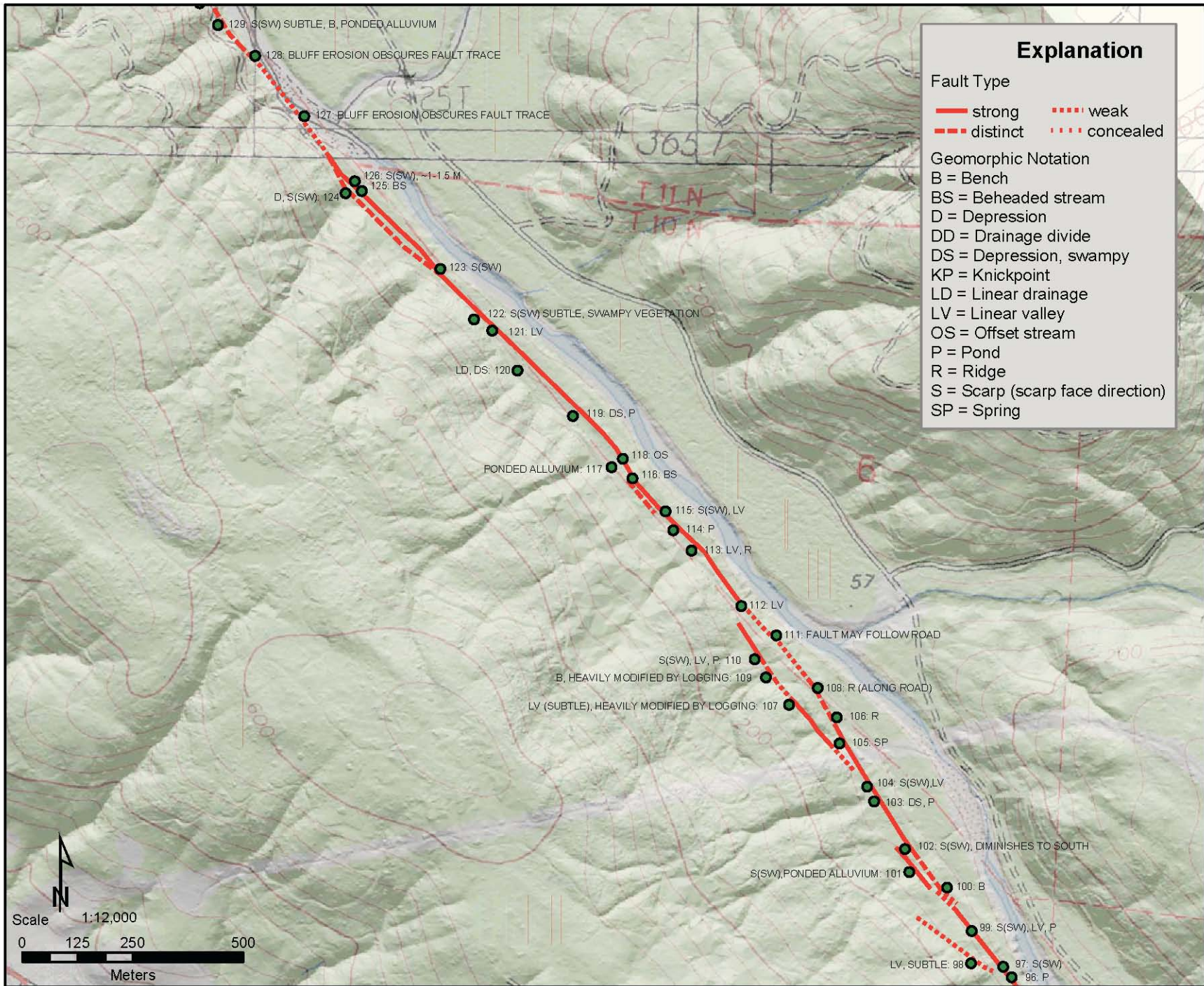


Figure 6d. Gualala River section of the San Andreas Fault. See Figure 7 for general location.

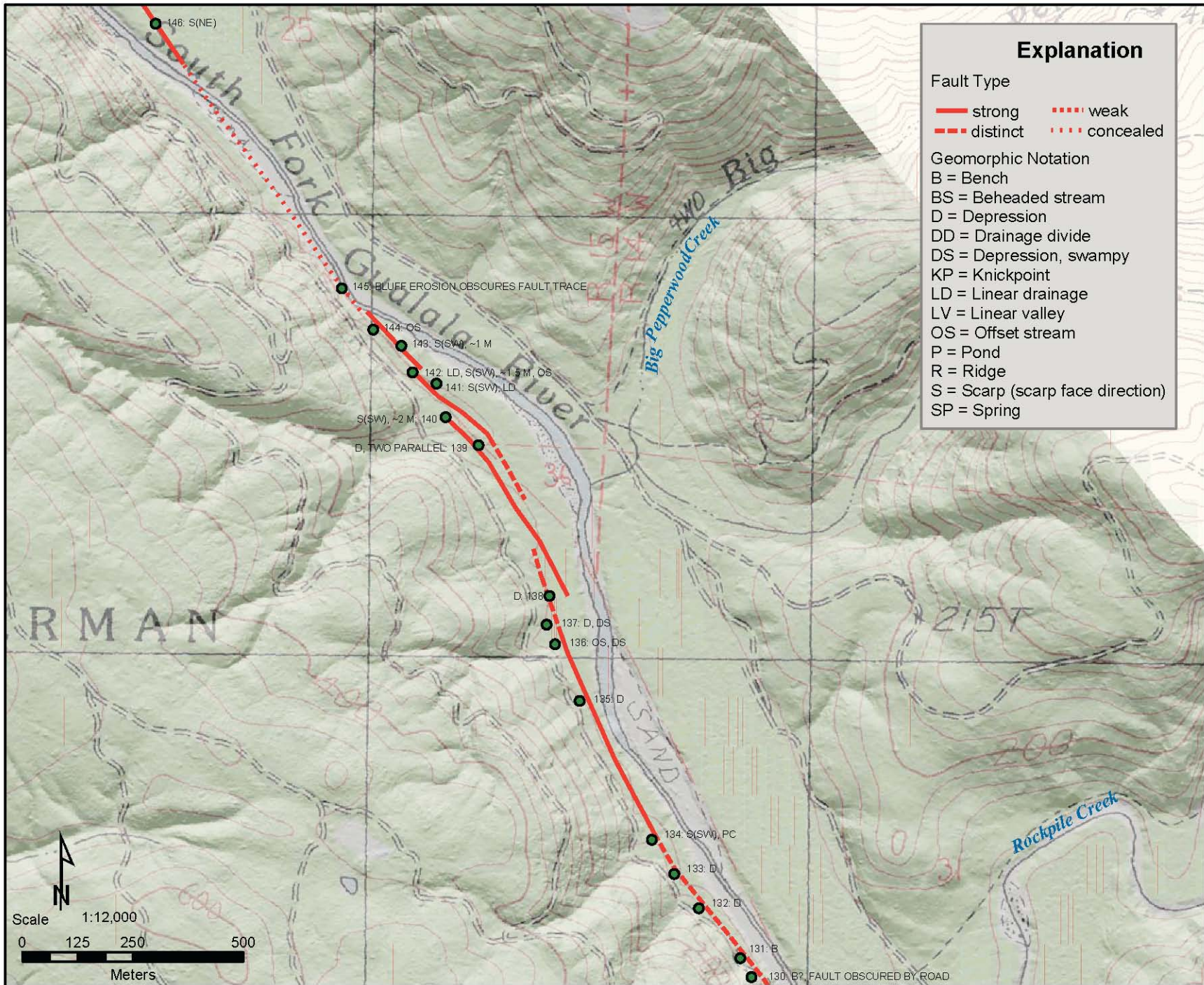


Figure 6e. Gualala River section of the San Andreas Fault. See Figure 7 for general location.

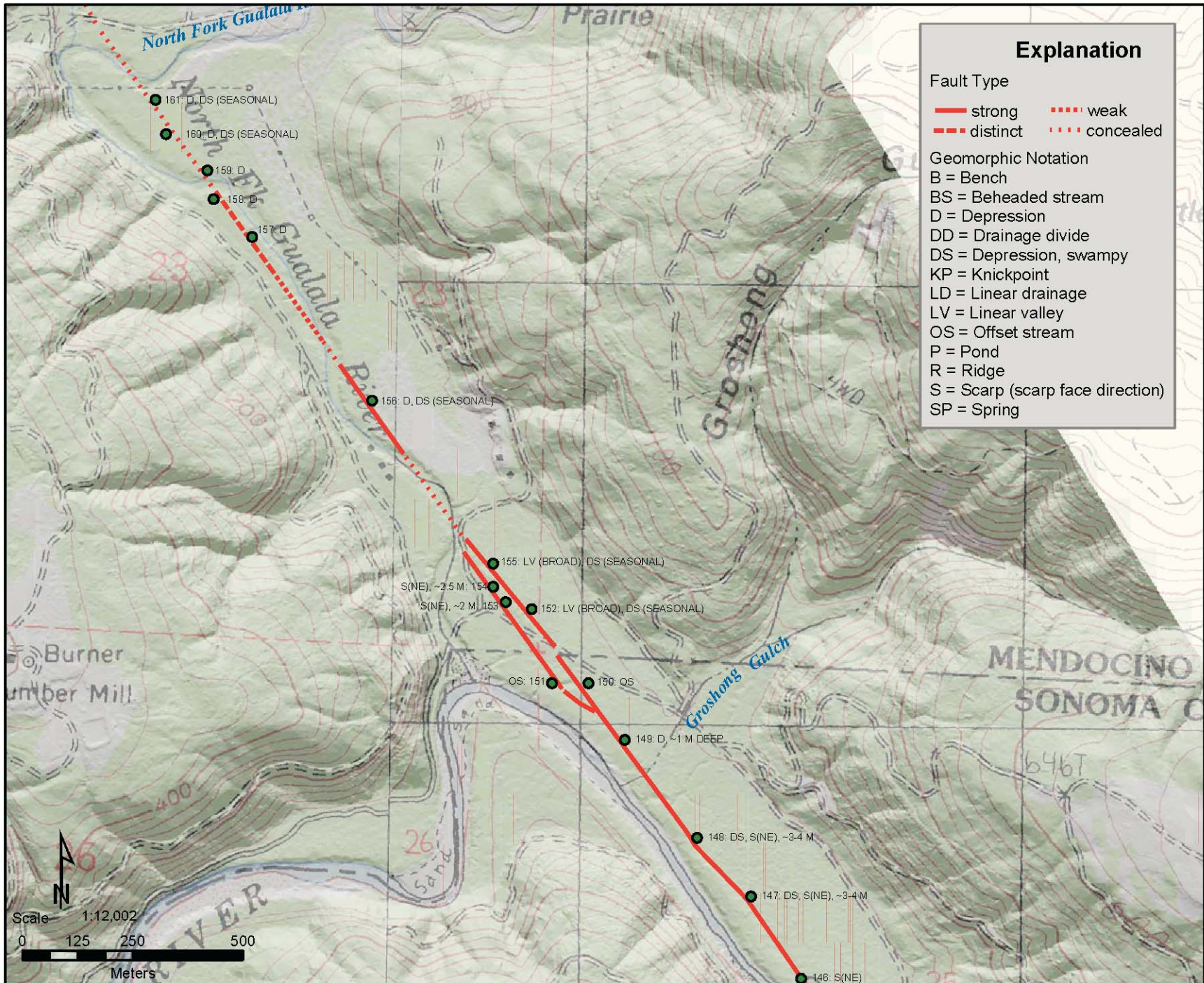


Figure 6f. Gualala River section of the San Andreas Fault. See Figure 7 for general location.

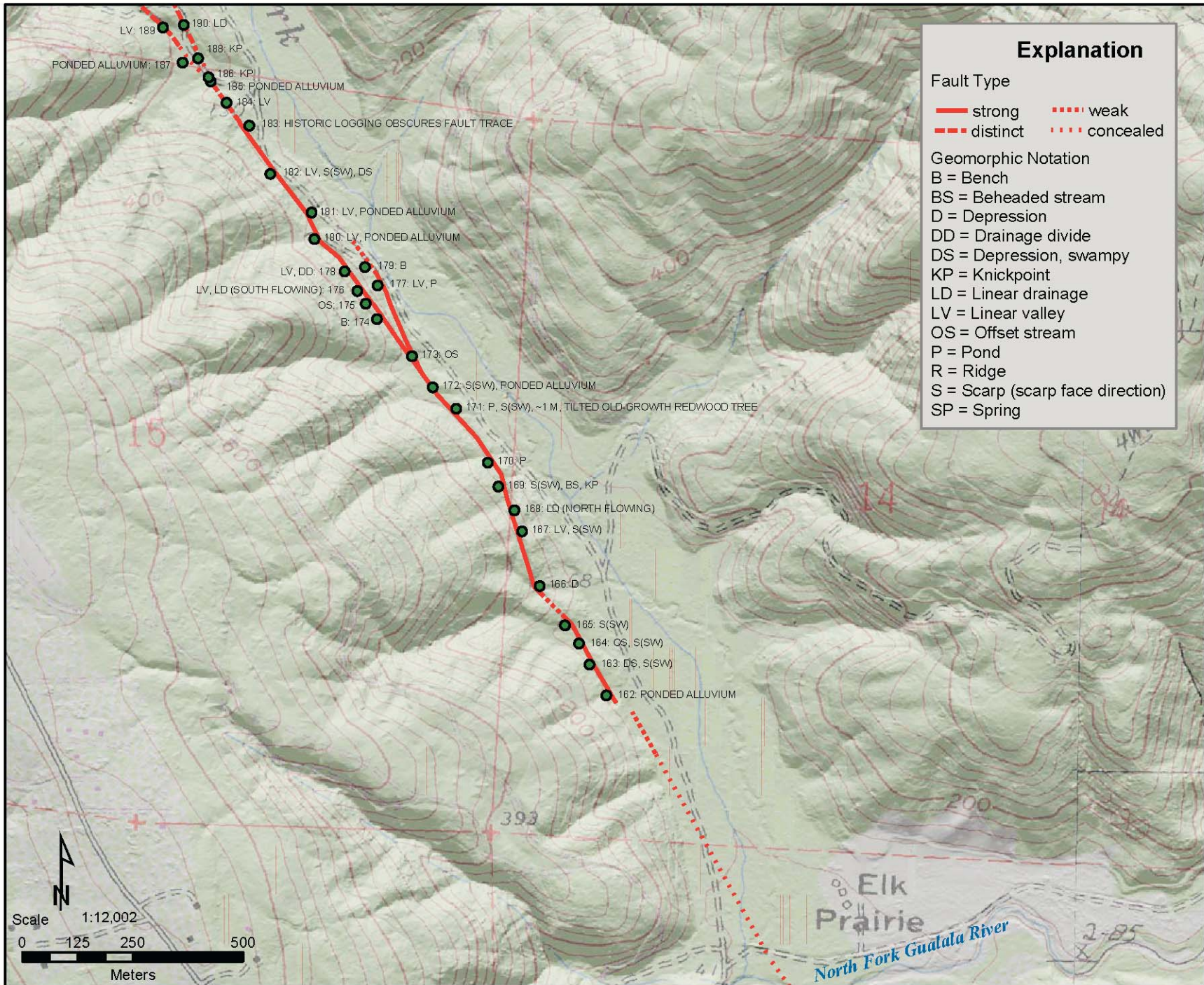


Figure 6g. Gualala River section of the San Andreas Fault. See Figure 7 for general location.

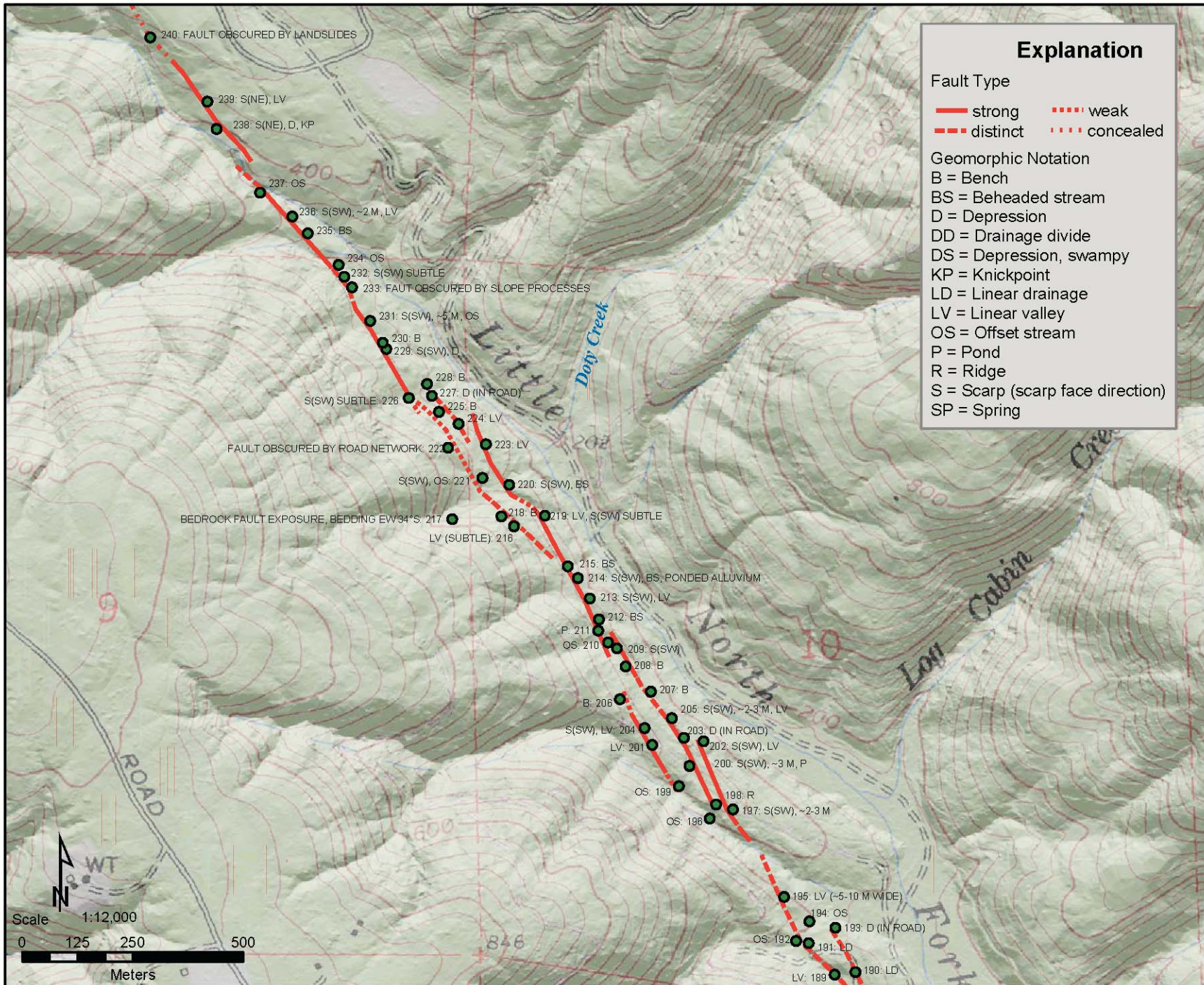


Figure 6h. Gualala River section of the San Andreas Fault. See Figure 7 for general location.

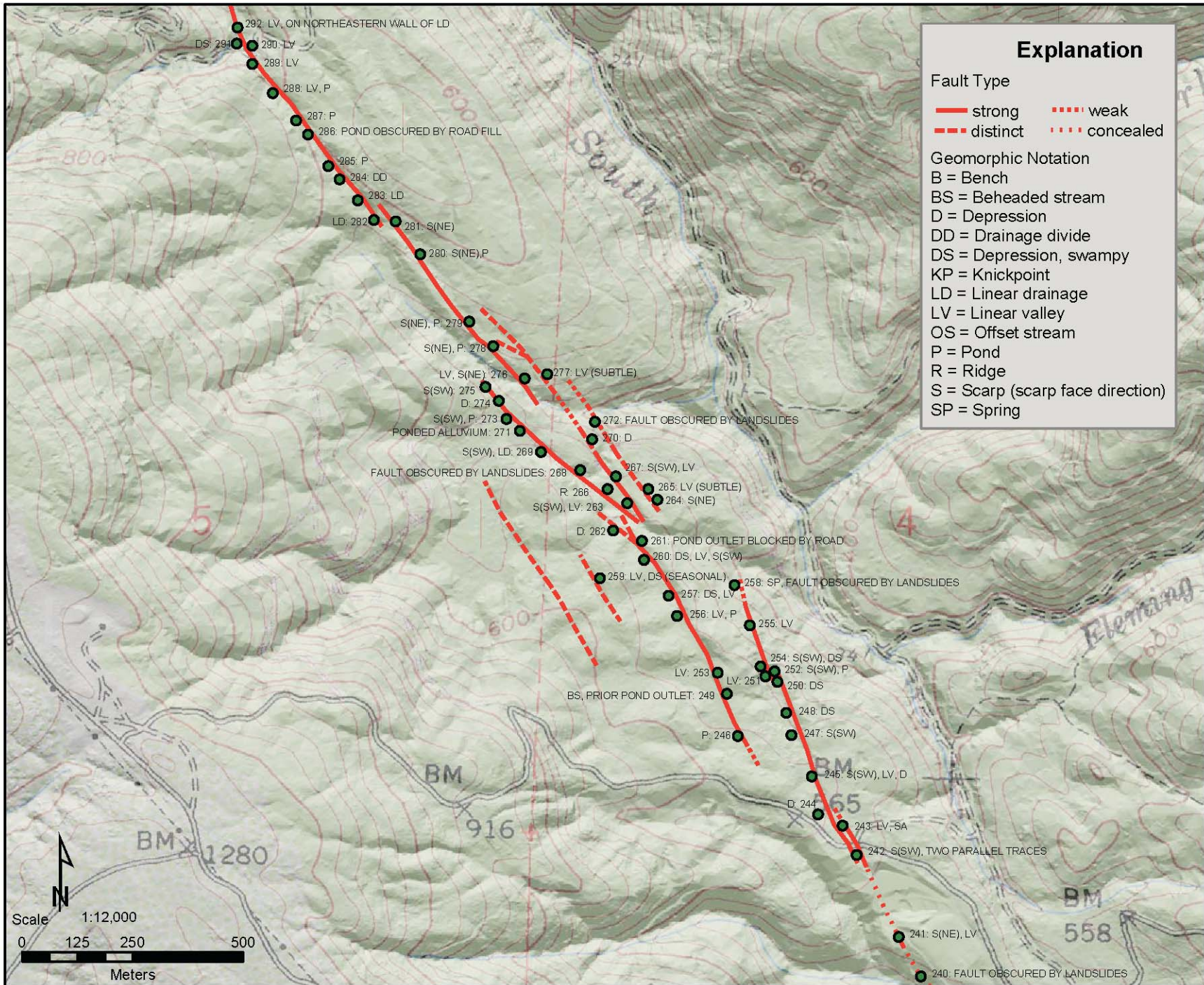


Figure 6i. Gualala River section of the San Andreas Fault. See Figure 7 for general location.

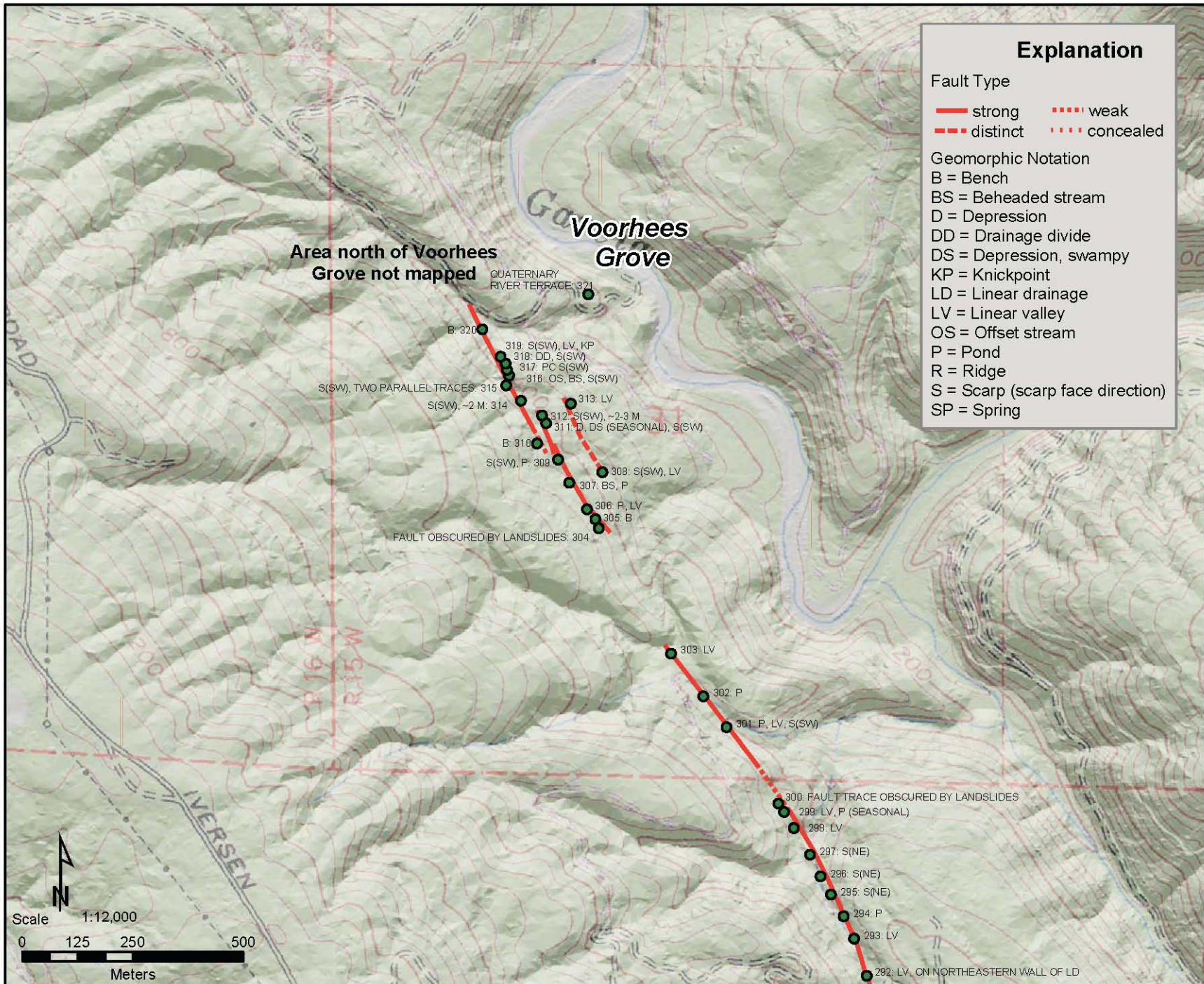


Figure 6j. Gualala River section of the San Andreas Fault. See Figure 7 for general location.

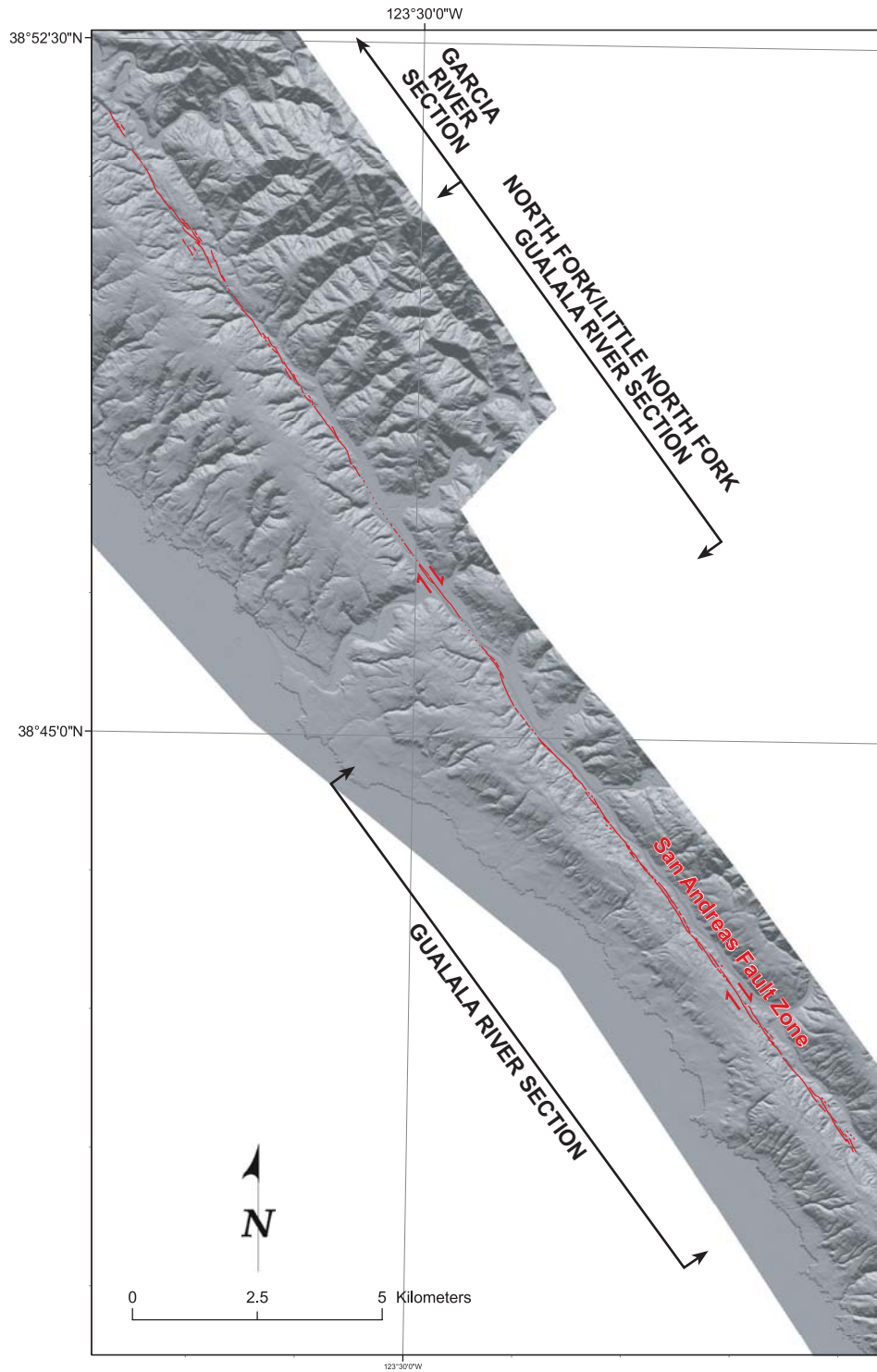


Figure 7. Location of geomorphic-related section boundaries along the 24-km-long field area of the Northern San Andreas fault.



Figure 8. Photograph, view to north-northeast, showing San Andreas fault at base of scarp on right adjacent to sag pond. Numerous large sag ponds exist along the fault in the Gualala River valley. A linear valley extends to the north. Photograph taken at site number 6.



Figure 9. A) Photograph, view northwest, showing redwood tree tilted on scarp of the 1906 rupture adjacent to a large sag pond. B) Close up of the base of tilted redwood tree showing possible deformation related to the 1906 rupture.



Figure 10. Photographs showing dense brush within a narrow linear valley along the trace of the San Andreas fault.